



1 Post-Disturbance Soil Monitoring in Forests using Remote

2 Sensing: An Evidence Map

3

4 Maisy Roach-Krajewski¹; Xavier Giroux-Bougard¹; David Paré¹; Catlan Dallaire²; Luc

5 Guindon¹; Florian Jordan¹; Charlotte Norris²; Kara Webster³; Jérôme Laganière¹

6 1. Centre de foresterie des Laurentides, Ressources naturelles Canada, Québec, G1V

7 4C7, QC, Canada

8 2. Pacific Forestry Centre, Natural Resources Canada, Victoria, V8Z 1M5, BC,

9 Canada

10 3. Great Lake Forestry Centre, Natural Resources Canada, Sault St. Marie, P6A 2E5,

11 ON, Canada

12

13 Correspondence to: Jérôme Laganière (jerome.laganiere@NRCan-RNCan.gc.ca)



14 **Abstract.** Forest soils underpin ecosystem resilience and productivity but are increasingly
15 threatened by natural and anthropogenic disturbances. Monitoring post-disturbance soil
16 degradation at operational scales remains challenging in forests, where ground-signal obstruction
17 and reliance on proxy indicators constrain remote sensing (RS) applications. To identify where
18 RS can benefit soil monitoring and support emerging reporting needs, we developed a structured
19 evidence map of studies assessing post-disturbance forest soil degradation using RS methods.
20 From 4,338 records, 72 primary studies were synthesized across disturbance types, biomes,
21 platforms, scales, and indicators. The evidence base is dominated by wildfire and harvesting,
22 reflecting disturbance pathways that produce observable surface impacts. Multispectral satellite
23 data remain the primary tool for mapping post-fire severity and erosion-related indicators, while
24 LiDAR and stereo-photogrammetry are most often used to quantify surface deformation after
25 harvest operations. Indicators tied to subsurface physical, chemical, or biological change remain
26 sparsely represented due to observability limits. Overall, RS is most effective for mapping
27 disturbance footprints, detecting surface-expressed indicators, and stratifying landscapes for
28 targeted field assessment, rather than directly measuring soil properties. This evidence map
29 clarifies the benefits and limits of RS, identifies persistent gaps, and highlights priorities for
30 developing disturbance-aware soil-monitoring frameworks. It also specifies which soil indicators
31 are defensibly observable with RS and which require complementary approaches. By linking
32 disturbance processes to observable indicators, this synthesis helps define realistic RS-supported
33 objectives for reporting frameworks within national forest monitoring and assessment programs.



34 1. Introduction

35 Forest soils underpin ecosystem productivity, hydrological regulation, and long-term resilience
36 following disturbance (e.g., Bonan, 2008; Paré et al., 2024; Pastore et al., 2025) , yet they remain
37 one of the least consistently monitored components of forest ecosystems. Physical, chemical, and
38 biological soil properties govern post-disturbance recovery trajectories, influence erosion and
39 nutrient loss, and condition forest responses to subsequent disturbances (Agbeshie et al., 2022;
40 Bowd et al., 2019; Schoenholtz et al., 2000). Not only are soils fundamental to forest health, but
41 they are also increasingly threatened and near irreplaceable. Soils are considered a non-
42 renewable resource that can require millennia to form, yet an estimated one-third of global soils
43 are already significantly degraded (Delgado-Baquerizo et al., 2025). Despite this importance, soil
44 degradation following disturbance is difficult to measure systematically, particularly at spatial
45 and temporal scales relevant to forest management (Delgado-Baquerizo et al., 2025; Pastore et
46 al., 2025).

47 Disturbances common to managed and unmanaged forests (e.g., wildfire, forest harvesting and
48 silvicultural treatments) can degrade soil structure, alter hydrologic behaviour, and disrupt
49 biogeochemical processes (Bowd et al., 2019; Cambi et al., 2015; Jordan et al., 2026). These
50 impacts are often spatially heterogeneous, occur at fine scales, and can persist long after above-
51 ground vegetation appears to recover (Bowd et al., 2019; DeArmond et al., 2021). In wildfire-
52 affected forests, the nature of soil impacts varies with fire intensity. High intensity crown fires
53 consume the understory and canopy, leaving behind charred standing dead trees. The forest floor
54 may also be burned, often in a patchy distribution . In contrast, low-intensity ground fires
55 typically burn only the understory, resulting in more limited alteration of soil surface conditions
56 (Brown et al., 2026). Variation occurs across forest-management disturbances as well. For



57 example, impacts on the forest soil depend on the type of harvesting approach used (e.g., clear
58 cut, partial cut) and subsequent silvicultural prescriptions for site preparation (e.g., blading, disc
59 trenching), residue management (residue piled, residue removed), vegetation control (e.g.,
60 herbicide application, free to grow) and regeneration approach (e.g., planting, natural
61 regeneration) (Brown et al., 2026). Collectively, the intensity and type of disturbance event
62 shape forest soil condition in distinct ways, underscoring the need for monitoring approaches
63 capable of capturing these nuances.

64 Traditional field-based soil monitoring provides essential, direct measurements of soil condition,
65 but logistical constraints limit spatial coverage and frequency across large or remote forest
66 landscapes (Maurya et al., 2020; Pastore et al., 2025). As a result, there is growing interest in
67 complementary approaches that can support landscape-scale assessment and prioritization.

68 Remote sensing (RS) has become a central tool for monitoring forest disturbance and recovery,
69 offering consistent, repeatable observations over large areas (Gao et al., 2020; Perbet et al.,
70 2025). In forestry, RS is widely used to map burned area and burn severity (Chen et al., 2024;
71 Perbet et al., 2025), track forest harvesting and regeneration (Perbet et al., 2025; White, 2024),
72 and characterize canopy structure and biomass (Borsah et al., 2023). Compared with agricultural
73 settings, where seasonal soil exposure enables more direct observation, forest RS applications
74 must contend with canopy and understory occlusion (Lausch et al., 2016; Weiss et al., 2020),
75 moisture-driven spectral variability (Ge et al., 2011; Weiss et al., 2020), and topographic effects
76 on illumination and temperature (Lausch et al., 2016; Quintano et al., 2019), which complicate
77 the translation of image- or point-cloud products into soil-specific interpretations. Nevertheless,
78 advances across optical, LiDAR, photogrammetric, thermal, and radar modalities, increasingly



79 used in combination, are expanding opportunities to support soil-relevant monitoring aims after a
80 disturbance (Gao et al., 2020; Nevalainen et al., 2017; Talbot and Astrup, 2021).

81 Although numerous studies have applied RS to assess post-disturbance forest soils, the literature
82 is disparate across disturbance types, sensor modalities, spatial scales, and indicator choices. Most
83 existing syntheses are either disturbance-specific (most often wildfire) or technology-specific
84 (e.g., LiDAR), which limits cross-comparison of methodological choices and the identification
85 of general patterns (e.g., Morgan et al., 2014; Talbot and Astrup, 2021; Venanzi et al., 2023).

86 This disparity makes it difficult to determine which RS approaches are appropriate for which
87 soil-monitoring objectives, which spatial and temporal scales are typical, and where major
88 validation demands and sources of uncertainty arise.

89 To address this gap, we developed a structured evidence map (Cook et al., 2017) of studies that
90 have applied RS to monitor post-disturbance soil degradation in forested landscapes,
91 synthesizing primary studies published between 1996 and 2025 across disturbance types, biomes,
92 sensor platforms, spatial and temporal scales, and soil-degradation indicators. Rather than
93 evaluating individual techniques in isolation, we organize the evidence base using a disturbance–
94 threat–indicator framework that links initiating disturbances to the soil degradation processes of
95 concern and to the surface expressions that RS can plausibly detect (observable vs. proxy-based
96 vs. limited) (Jordan et al., 2026).

97 Monitoring post-disturbance soil change is not only a scientific objective but also a reporting
98 requirement for many forest agencies. To meet these obligations, land-management authorities
99 must translate diverse soil impacts into indicators that are measurable, comparable through time,
100 and defensible under external review. At the global scale, the FAO Global Forest Resources



101 Assessment (FAO, 2025) reinforces the importance of such standardized, indicator-driven
102 approaches for national- and global-scale forest reporting.

103 Accordingly, this evidence map aims to: (i) describe the scope and distribution of RS
104 applications for post-disturbance soil indicators across disturbance contexts and forest biomes;
105 (ii) identify patterns linking disturbance type, soil threats, indicator selection, and RS design
106 choices; and (iii) evaluate which RS-observable indicators are most defensible for national
107 monitoring and reporting, clarifying strengths, limitations, and validation demands for
108 operational uptake.

109 2. Methods

110 2.1 Publication search

111 Following the guidelines for conducting evidence maps in environmental sciences (Collaboration
112 for Environmental Evidence, 2022), we composed a search string to capture publications that
113 assessed indicators of post-disturbance soil degradation in forests using RS techniques (see
114 Appendix Table A1). This search string was used to query titles, keywords, and abstracts of
115 relevant publications, which included journal articles, but also grey literature such as conference
116 proceedings, theses, and reports. We used Scopus, EBSCO host, and OpenAlex databases to
117 access and extract relevant publications between the 25th and 26th of February 2025. We also
118 used the same search string to query Google Scholar and retrieved the first 300 publications
119 ranked by relevance using the Publish or Perish software (Harzing, 2007). To include published
120 government reports not represented in the bibliographical databases, we expanded our search to
121 government repositories including Québec's MFFP archive, Ontario's MNRF archive, Natural



122 Resource Canada’s Open Science and Technology repository (OSTR), and the United States
123 Forest Service Tree Search repository. Only English and French records were retained across all
124 databases.

125 2.2 Screening and eligibility

126 After extracting the raw search results from the bibliographical database searches, we parsed
127 them into a common format using the “*tidyverse*” collection of packages (Wickham et al., 2019)
128 implemented in R (R Core Team, 2024). Then, we screened the parsed results to identify and
129 remove duplicate records by flagging any pairwise similarity of titles and authors.

130 To be retained for further inspection, a relevant publication had to meet the following four
131 eligibility criteria: 1) use RS methods to analyze post-disturbance soil degradation in a forested
132 area; 2) draw direct (e.g., in-situ measurement) or indirect (e.g., photointerpretation) links
133 between RS measurements or products and in-situ indicators of soil degradation; 3) be conducted
134 after a disturbance (i.e., simulation/predictive models and risk assessments were excluded); and
135 4) contain sufficient methodological details (e.g., sensor specifications, data processing steps,
136 and validation methods) to understand how RS products were used. Relevant reviews were
137 excluded from the primary set but retained for the snowball search (Section 2.3).

138 Publications that ‘passed’ the initial title/abstract screening or were deemed ‘inconclusive’ based
139 on title/abstract alone were followed up with a full-text screening, to verify that all criteria were
140 met. Screening was performed by a single reviewer for consistency.

141 2.3 Snowball search



142 To complement the initial database search, we used a snowball search method to examine the
143 references (backward snowballing) and citations (forward snowballing) of a set of input
144 publications (i.e., screened-in studies and relevant reviews). To facilitate this process, we used
145 *Research Rabbit* (<https://www.researchrabbit.ai>), a web-based tool that visualizes citation
146 networks and thematic relationships, and recommends related papers based on an initial set of
147 publications. Newly found records were screened against the same criteria by a second reviewer,
148 and duplicates were removed before extraction.

149 2.4 Data extraction and coding

150 For each relevant primary study (excluding review articles), we extracted detailed information on
151 study location, sample size, forest and soil characteristics, types and dates of disturbances,
152 observed outcomes, and the soil degradation indicators used. We also extracted the types of
153 sensors used in the study, associated RS methods (e.g., platform types, metric indices,
154 classification, and validation techniques), in-situ indicators used for ground-truthing, study
155 design, objectives, and overall conclusions. To streamline analysis, we grouped soil indicators
156 into broader categories. This process involved: extracting all unique recorded values, correcting
157 typos and merging redundant terms (e.g., “organic soil depth” and “depth of organic soil”), and
158 identifying similar (e.g., “soil moisture content” and “soil water content”) and nested terms (e.g.,
159 “rut depth” and “rut volume” under “rut severity”). We then iteratively defined each broader
160 category to encompass these groupings or distinct standalone terms. Field experts then reviewed
161 the resulting categories, definitions, and grouped terms to validate their accuracy and relevance.
162 Finalized categories can be found in the Appendix (Table A2).



163 To examine the scope and distribution of the evidence base, including temporal trends and
164 biogeographical coverage, as well as variations within and across disturbance types and RS
165 methods, we organized and visualized the compiled data in R (version 4.1.3; R Core Team,
166 2024) using packages including *sf* (Pebesma, 2018), *ggplot2* (Wickham et al., 2016),
167 *naturalearth* (Massicotte et al., 2025), *forcats* (Wickham et al., 2025a), *stringr* (Wickham, 2010),
168 *googlesheets4* (Bryan, 2025), and *scales* (Wickham et al., 2025b).

169 3. Results

170 3.1 Overview of evidence base

171 3.1.1 Publication details

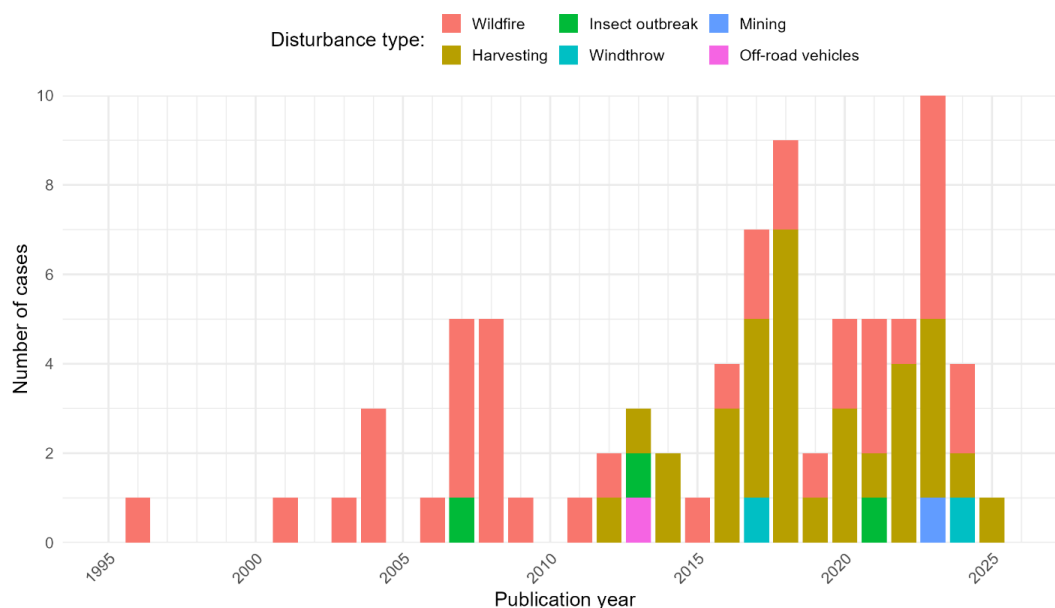
172 Our database search yielded 3,256 publications for screening. After applying the eligibility
173 criteria described in Section 2.2, we retained 64 publications and 6 relevant review papers. These
174 70 publications were then used to conduct a snowball search, which retrieved an additional 1,082
175 distinct publications, for a total of 4,338 publication. Screening of these snowball search results
176 identified 8 more eligible studies, resulting in a final evidence base of 72 publications
177 (Appendix, Figure A1).

178 3.1.2 Disturbance types

179 The evidence base captures six types of disturbances: wildfire (n = 39/77; 50.6%), harvesting (n
180 = 33/77; 42.9%), insect outbreak (n = 2; 2.6%), windthrow (n = 2; 2.6%), mining (n = 1; 1.3%),
181 and off-road vehicle use (n = 1; 1.3%). Here, “harvesting” is used as an umbrella term for a
182 range of harvesting practices represented in the evidence base, including clear-cutting, partial
183 cutting, cut-to-length operations, thinning, skidding, selective harvesting, and salvage harvesting.



184 Most publications (n = 66/72, 91.7% of evidence base) assessed the aftereffects of only one
 185 disturbance type. Among the six studies that addressed multiple disturbance types, five involved
 186 salvage harvesting after a wildfire (n = 3; 4.2%), insect outbreak (n = 1; 1.4%), or windthrow (n =
 187 1; 1.4%) event. Post-wildfire studies provide the most consistent coverage across the temporal
 188 span of the evidence base (1996-2025), with at least one publication in 20 of the 29 years since
 189 the first case in 1996. In contrast, the first study involving harvesting, the second most frequently
 190 recorded disturbance, was published over a decade later in 2012 (Figure 1).



191

192 **Figure 1:** Disturbance type frequency by publication year. Each bar shows the annual sum of disturbance
 193 cases reported across studies. Overall disturbance type totals were: Wildfire (39); Harvesting (33); Insect outbreak
 194 (3); Windthrow (2); Mining (1); Off-road vehicles (1).

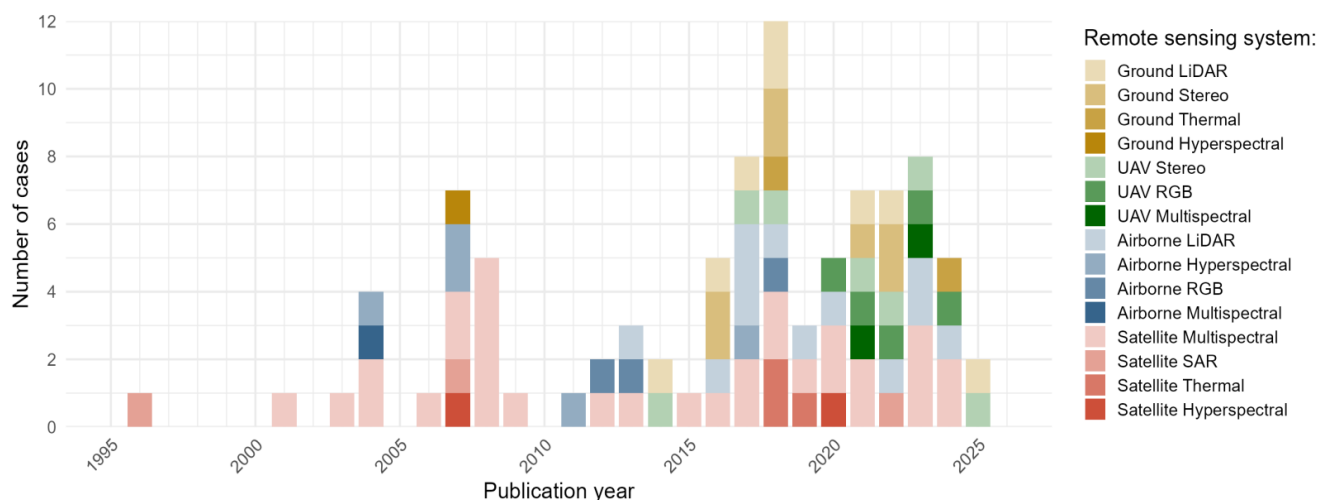
195

196 *3.1.3 Remote sensing technologies*

197 Multispectral sensors were the most used sensor type (n = 34; 37.0%), followed by LiDAR (n =
 198 20; 21.7%) and stereo photogrammetric data (n = 14; 15.2%). Satellite platforms were used most



199 frequently (n = 39; 42.4%), paired with multispectral sensors (n = 31; 33.7%) (Figure 2).
 200 Satellite-based sensors provide the most consistent coverage across the temporal span of the
 201 evidence base (1996-2025), while sensors using unmanned aerial vehicles (UAV) only appeared
 202 in the literature after 2013 (Figure 2). *Platform-sensor combinations by disturbance are shown in*
 203 *Appendix Figure A2*. A single platform type was used in most studies (n = 59; 81.9%), whereas
 204 13 studies used more than one type. Analytically, studies most often used spectral index-based
 205 analysis (n = 29; 31.9%), LiDAR-specific analyses (n = 19; 20.9%), image differencing (n = 17;



206 18.7%), and photogrammetry (n = 17; 18.7%) (Appendix, Figure A3). Only 10 studies (13.9%)
 207 combined multiple approaches, with the rest of the studies (n = 62; 86.1%) using only one.

208 **Figure 2:** Stacked counts of platform-sensor combinations by publication year. Note that a single study
 209 could contain more than one platform-sensor combination. Total counts for platform sensor combinations
 210 were: satellite Multispectral (31); airborne LiDAR (12); ground LiDAR (8); ground Stereo (7); UAV
 211 Stereo (7); UAV RGB (5); airborne Hyperspectral (5); airborne RGB (3); satellite SAR (3); satellite
 212 Thermal (3); ground Thermal (2); UAV Multispectral (2); satellite Hyperspectral (2); ground
 213 Hyperspectral (1); airborne Multispectral (1).

214



215 *3.1.4 Study locations*

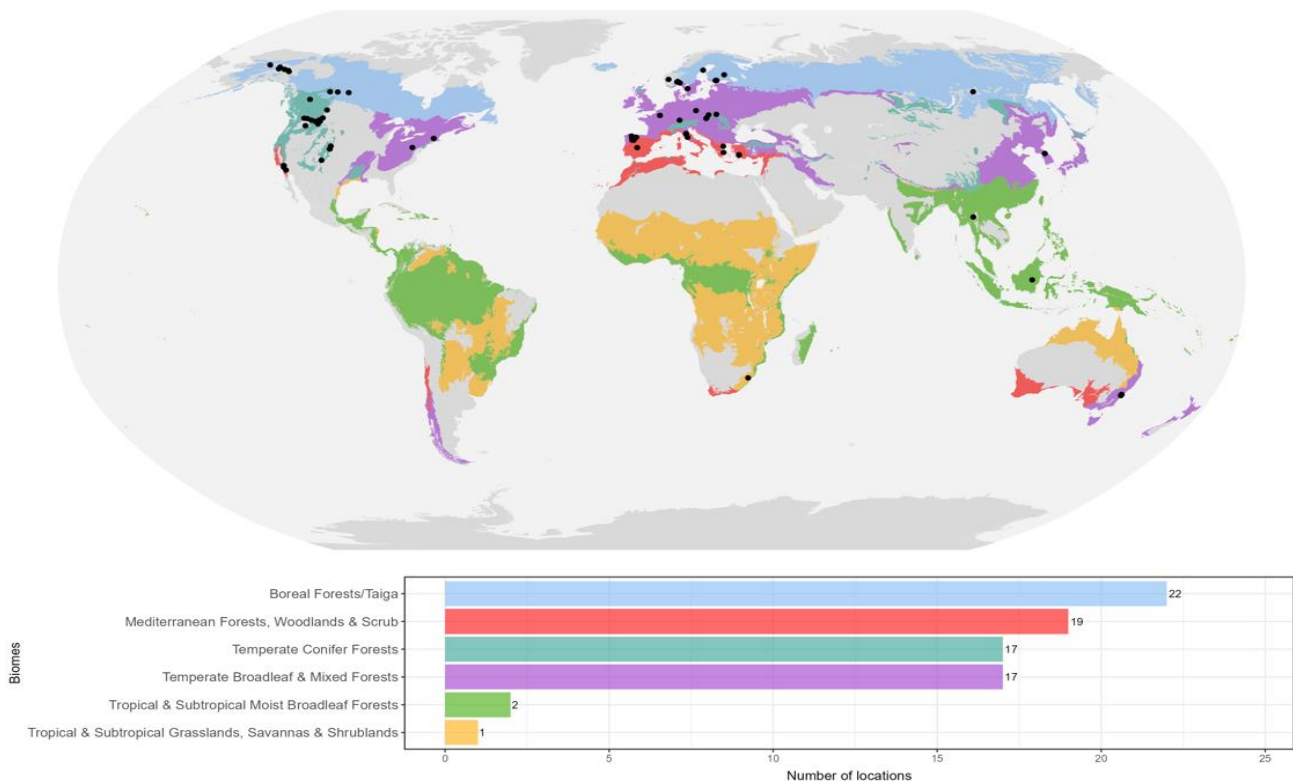
216 Although our search placed no restrictions on country of origin, the majority of studies included
217 were carried out in European (n = 37; 51.4%) or North American (n = 27; 37.5%) forests (Figure
218 3). Collectively, the evidence base spans four of the seven global forested biomes and two of the
219 seven non-forested biomes (Dinerstein et al., 2017). Most studies occurred in boreal forests/taiga
220 (n = 22; 28.2%), followed by Mediterranean forests and woodlands (n = 19; 24.4%), temperate
221 conifer forests (n = 17; 21.8%), and temperate broadleaf and mixed forests (n = 17; 21.8%).
222 There were two cases of tropical and subtropical moist broadleaf forests (n = 2; 2.6%), and one
223 of tropical/subtropical grassland (n = 1; 1.3%) within a eucalypt plantation in South Africa. This
224 was the only case outside a naturally occurring forest (Figure 3). Most studies (n = 67; 93.1%)
225 were conducted within a single biogeographic area, meaning all assessments took place within



226 forests of the same terrestrial biome. Four studies included two biomes each, and one study

227 (Hudak et al., 2007) included three.

228 **Figure 3.** Map of the study locations (n = 78) across included publications (n = 72) relative to the world's
229 terrestrial biomes (data source: Dinerstein et al., 2017). Bar chart below shows the number of study
230 locations by biome.





231 3.2 Patterns in study design and methodology

232 3.2.1 Sensor use by biome within different disturbance contexts

233 Across 106 biome \times disturbance \times sensor cases, the most frequent biome-disturbance pairings
234 were: wildfire in Mediterranean forests (n = 22; 20.8%), wildfire in temperate conifer (n = 14;
235 13.2%), harvesting in boreal/taiga (n = 14; 13.2%), and harvesting in temperate broadleaf/mixed
236 (n = 11; 10.4%) (Figure 4). By disturbance-sensor pairing, multispectral sensors post-wildfire
237 were most common (n = 32; 30.2%), whereas LiDAR (n = 14; 13.2%) and stereo
238 photogrammetry (n = 13; 12.3%) were most used post-harvesting. By biome-sensor pairing,
239 multispectral dominated in Mediterranean (n = 14; 13.2%), temperate conifer (n = 11; 10.4%),
240 and temperate broadleaf/mixed (n = 8; 7.5%); in boreal/taiga, stereo (n = 7; 6.6%) and
241 multispectral (n = 7; 6.6%) were co-dominant. The most frequent three-way combinations were
242 multispectral for wildfire in Mediterranean (n = 13; 12.3%), stereo for harvesting in boreal/taiga
243 (n = 7; 6.6%), multispectral for wildfire in temperate conifer (n = 7; 6.6%), and multispectral for
244 wildfire in temperate broadleaf/mixed (n = 6; 5.6%) (Figure 4).



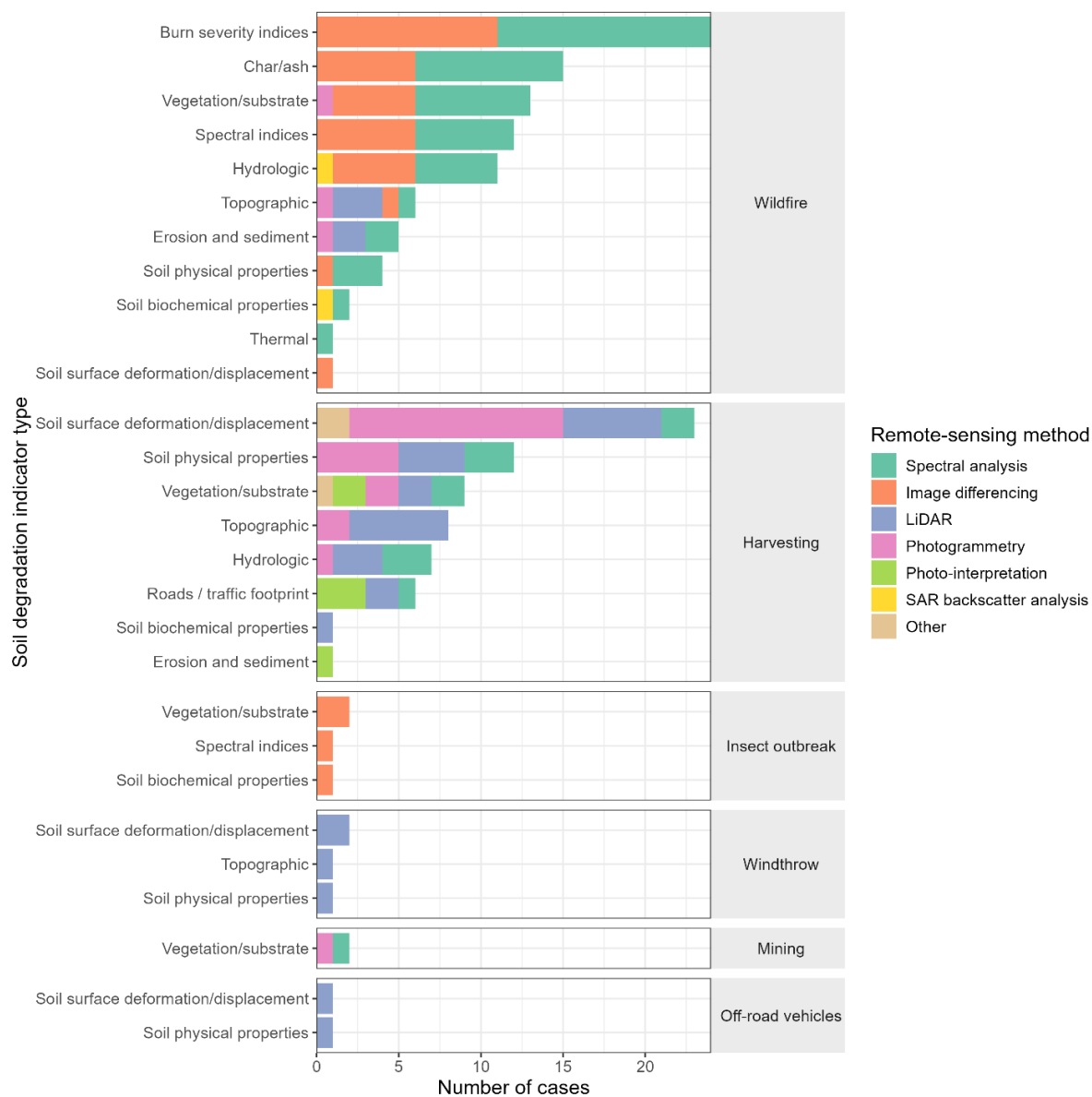
245 **Figure 4:** Number of cases of each sensor type use across biomes, separated by disturbance type. Note
 246 that a single study could have more than one biome, sensor type, or disturbance type recorded, thus each
 247 combination of biome, sensor type, and disturbance type is counted as one “case” (106 cases across 72
 248 studies).



249 *3.2.2 Indicators and remote sensing methods*

250 Across 173 indicator x method x disturbance cases, the leading indicator–disturbance pairs were:
251 burn severity and wildfire (n = 24; 13.9%), soil surface deformation/displacement and harvesting
252 (n = 23; 13.3%), char/ash and wildfire (n = 15; 8.7%), vegetation/substrate and wildfire (n = 13;
253 7.5%), soil physical properties and harvesting (n = 12; 6.9%), and spectral indices and wildfire
254 (n = 12; 6.9%) (Figure 5). Across indicator-method pairings, burn severity indices were
255 predominantly derived from spectral analysis (n = 13; 7.5%) and image differencing (n = 11;
256 6.4%), whereas soil surface deformation/displacement measurements were most often obtained
257 from photogrammetry (n = 13; 7.5%) and LiDAR (n = 9; 5.2%). Topographic measurements
258 relied mainly on LiDAR (n = 10; 5.8%), and vegetation/substrate measurements were typically
259 quantified using spectral analysis (n = 10; 5.8%) or image differencing (n = 7; 4%).
260 Correspondingly, spectral analysis and image differencing dominated wildfire applications (n =
261 48; 28%, and n = 36; 21%, respectively), while harvesting assessments relied primarily on
262 LiDAR (n = 24; 14%) and photogrammetry (n = 23; 13%). Overall, the most frequent
263 combinations for indicator-disturbance-method were burn severity indices derived from spectral
264 analysis in wildfire studies (n = 13; 7.5%) and soil surface deformation/displacement
265 measurements derived from photogrammetry in harvesting contexts (n = 13; 7.5%). Additional
266 RS methods combinations are shown in Appendix Figure A3.

267



268 **Figure 5:** Number of cases of each remote-sensing method used across soil degradation indicator type,
 269 separated by disturbance type. Soil degradation indicator type classifications are summarized in Table A2.
 270 Note that a single study could have more than one degradation type, remote-sensing method, or
 271 disturbance type recorded, thus each combination of degradation type, remote-sensing method, or
 272 disturbance type is counted as one “case” (173 cases across 72 studies).



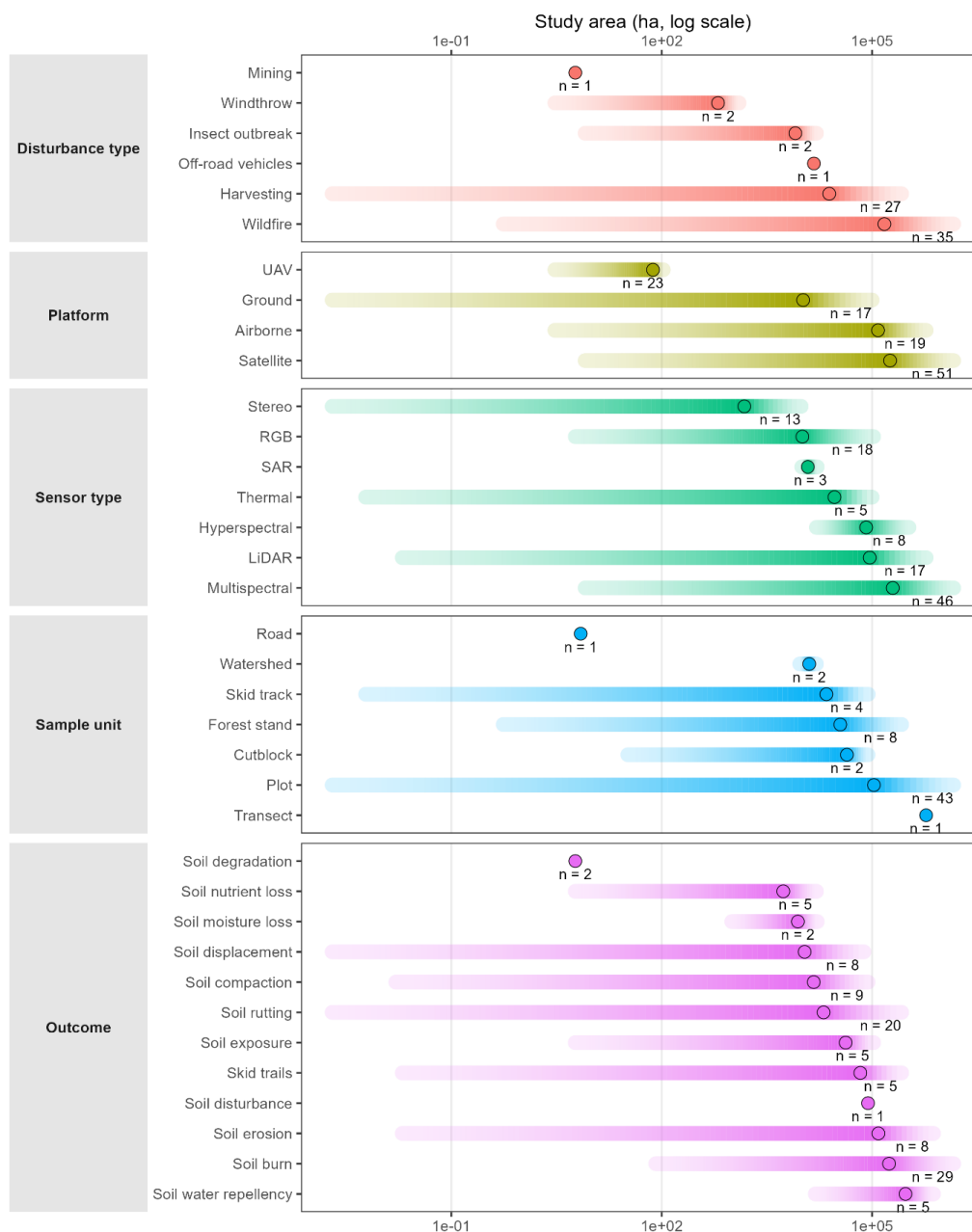
273 *3.2.3 Spatial scale*

274 Across the 62 studies with reported study area (i.e., full area of undertaking assessed by RS
275 tools), the spatial extent of assessments ranged from 0.002 to 1,455,268 ha (median = 10,858 ha,
276 mean = 91,137 ha), with a harvesting study holding the smallest study area, and a wildfire study
277 holding the largest (Figure 6). Wildfire cases (most frequent, n = 35; 56.5%) had the largest
278 extents (mean 149,665 ha; range 0.55-1,455,268 ha). Harvesting cases (n = 27; 43.5%) spanned
279 smaller but variable extents (mean 24,513 ha; range 0.002-263,900 ha). Insect and windthrow
280 were fewer (n = 2; 3.2% each) and smaller (mean 8,045 and 636 ha), while the single mining
281 case averaged 5.9 ha. By platform, satellite (n = 51; 46.4% of platform-type cases) covered 8.1 to
282 1,455,268 ha (mean 180,508 ha); UAV (n = 23; 20.9%) covered 3.0 to 105.3 ha (mean 75.2 ha);
283 ground ranged 0.002 to 100,000 ha (mean 10,396 ha). By sensor, multispectral (n=46; 41.8% of
284 sensor-type cases) averaged 106,110 ha (range 8.1-1,455,268 ha), while stereo (n=13; 11.8%)
285 had the lowest mean (1,509 ha) but the broadest range (0.002-9,726 ha). Soil burn (n=29; 29.3%
286 of outcome-type cases) and soil erosion (n=8; 8.1%) were often mapped over large to very large
287 extents (means of 174,660 and 123,021 ha, with maximum areas up to 1,455,268 and 750,000 ha,
288 respectively), whereas soil rutting (n=20; 20.2%), compaction (n=9; 9.1%), and displacement
289 (n=8; 8.1%) tended to be evaluated at intermediate scales (means of 20,339, 14,712, and 10,919
290 ha) with broad ranges. Plots were the most common sampling unit (n = 43; 70.5% of sample
291 unit-type cases) and spanned 0.002 to 1,455,268 ha (mean 106,110 ha); a single transect study
292 (n=1; 1.6%) had the largest mean (589,552 ha).

293 To represent the remote-sensing mapping scale rather than field-sampling scale, Figure 6 uses
294 the larger reported area as study extent. This choice captures the scope at which RS characterized
295 disturbance patterns but yields broad ranges, especially for ground platforms that were applied



296 only to subsets of larger areas mapped with satellite or airborne data. Consequently, spatial
 297 patterns in Figure 6 should be treated as approximate indicators of monitoring design, with
 298 comparisons informed by both mean values and the full range of reported extents.



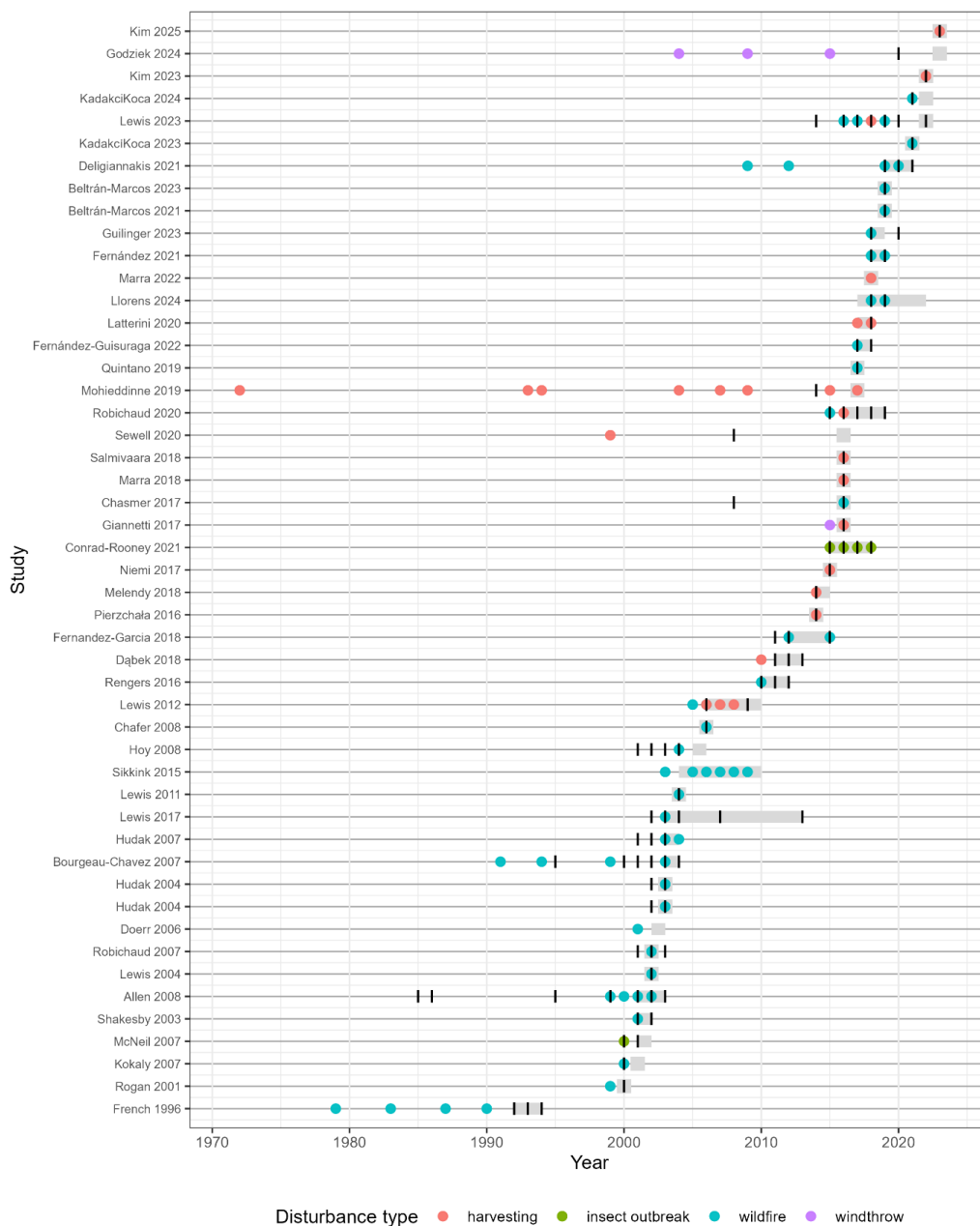


299 **Figure 6:** Spatial extent of included studies which reported study area ($n = 62$), according to disturbance
300 type, platform type, sensor type, sample unit, and soil degradation outcome. Each horizontal bar shows
301 the area of interest for a given category, with the gradient indicating the range from minimum to
302 maximum study area, with the black circle marking the mean. Values are plotted on a \log_{10} scale. Note
303 that a single study could have more than one disturbance type, platform type, sensor type, or outcome
304 recorded, thus each unique combination is counted as one “case”, denoted by n .

305

306 *3.2.4 Temporal patterns for disturbance events, RS acquisition, and data collection*

307 Of the 72 studies in the evidence base, 49 (68.1%) provided enough detail on sampling years
308 (i.e., data collection) and disturbance timing to allow assessment of temporal patterns. Across
309 these studies, we identified 92 disturbance events: wildfires were most common ($n = 57$; 62.0%),
310 followed by harvesting ($n = 26$; 28.3%), insect outbreaks ($n = 5$; 5.4%), and windthrow ($n = 4$;
311 4.3%) (Figure 7). Fifteen studies (30.6%) recorded multiple events of the same type (11 of which
312 were wildfires). RS acquisition years were reported in 46/49 timing-eligible studies (93.9%), and
313 40/46 (87.0%) included at least one acquisition year matching a disturbance year. The longest
314 minimum post-disturbance lag between disturbance timing and RS acquisition was 9 years
315 (harvesting in 1999 with RS acquisition in 2008; Sewell et al., 2020). Pre-disturbance RS was
316 reported in 10 studies (20.4%), all of which were for wildfire cases. The mean minimum
317 disturbance-to-sampling difference was 3.1 years (median 0). The largest gap between
318 disturbance and sampling period was 45 years (historical event used for multi-decadal recovery),
319 followed by 17 years (harvesting case). Sampling periods took place over one year or more in
320 60% of studies, with the longest spanning 10 years (2003-2013). RS acquisition typically
321 coincided with sampling: 65% of RS acquisition years fell within sampling windows and 82% of
322 studies used at least one RS acquisition during sampling. When acquisition and sampling did not
323 overlap, acquisition more often preceded sampling (33 years) than followed it (2 years), with the
324 largest offset 16 years (acquisition 1985; sampling 2001-2003) (Figure 7).



325 **Figure 7:** Timeline of disturbance events, RS acquisition, and sampling (i.e., data collection) periods for
 326 all studies with sufficient timing information (n = 49). Each row represents a single study; grey squares
 327 and horizontal bars show the year(s) that sampling took place, black tick marks represent the years
 328 associated with RS acquisition, and coloured points mark the years of disturbance events, identified by
 329 type.



330 4. Discussion

331 4.1 Disturbance contexts and observability

332 Across the evidence base, RS of post-disturbance soil degradation is not approached as a single
333 measurement. Instead, methods are selected (and validated) in relation to the disturbance-threat
334 pathway that makes soil degradation observable (Kubiak et al., 2024; Talbot et al., 2018).
335 Disturbances that produce widespread canopy loss and altered surface reflectance (e.g., wildfire)
336 (Lewis et al., 2011; Llorens et al., 2024; Veraverbeke et al., 2018) or mechanically induced
337 surface deformation (e.g., forest operations) (Nevalainen et al., 2017; Pierzchała et al., 2016;
338 Talbot and Astrup, 2021) dominate because they create signals that RS can detect with
339 comparatively high confidence. This section summarizes how these dominant contexts shape the
340 structure of the evidence base and the interpretability of RS-derived soil indicators.

341 *4.1.1 Dominant disturbance pathways*

342 Wildfire and harvesting dominate the evidence base, whereas insect outbreaks, windthrow,
343 mining, and off-road vehicle use are sparsely documented reflecting an imbalance in research
344 priorities and fundamental differences in observability. After wildfire, the combination of canopy
345 loss, surface exposure, and combustion residues produces clear spectral signals that multispectral
346 sensors can detect over large areas, enabling rapid assessment using spectral indices and
347 pre/post-fire differencing (e.g., Hudak et al., 2004; Shakesby et al., 2003). The depth of satellite
348 archives further enables disturbance-proximal analyses and helps explain the persistent
349 representation of wildfire studies across nearly three decades (Kokaly et al., 2007).



350 By contrast, soil impacts from mechanized harvesting are spatially discontinuous (e.g., tracks,
351 ruts, landings, localized displacement) and often obscured by slash and residual canopy,
352 increasing dependence on very-high-resolution imagery and/or 3D surface reconstruction (Talbot
353 and Astrup, 2021). These requirements constrain geographic coverage and sample sizes relative
354 to fire studies. Consistent with this pattern, harvesting-focused studies most commonly employ
355 close-range terrestrial, airborne, or UAV platforms, and rely on LiDAR or stereo-
356 photogrammetry to resolve traffic footprints (e.g., Bhatnagar et al., 2022) and quantify surface
357 deformation via terrain modelling (DTM differencing or point-cloud change; Venanzi et al.,
358 2023).

359 Unlike prior syntheses that are disturbance-specific (often wildfire) or technology-specific (e.g.,
360 LiDAR), this review assembles multiple disturbance contexts within one evidence map, enabling
361 direct comparisons of observability, indicator selection, and scale. This integrated perspective
362 also reveals diverging uptake trajectories, with wildfire applications recurring across nearly three
363 decades, whereas harvesting studies appear only after 2012 and remain comparatively
364 intermittent.

365 *4.1.2 Compound and stacked disturbances*

366 A smaller but important subset of the evidence base addresses compound disturbances, most
367 often salvage harvesting following wildfire. Stacked sequences complicate RS by requiring
368 attribution across overlapping temporal signals and by narrowing the window during which soil-
369 relevant surface expressions remain detectable. Detection accuracy declines rapidly as vegetation
370 regrowth and slash obscure signals, making disturbance-proximal acquisition critical. Further,
371 fine spatial resolution is frequently required to separate salvage-related soil disturbance from fire
372 effects (Dubé and Berch, 2013; Lewis et al., 2012). When timing and resolution are adequate,



373 optical indices, high-resolution imagery, and LiDAR can jointly support attribution by separating
374 vegetation recovery patterns from mechanically induced surface change (Giannetti et al., 2017;
375 Lewis et al., 2023; Robichaud et al., 2020). Evidence also indicates that stacked disturbances are
376 non-additive: salvage can amplify erosion risk, increase connectivity along trail networks, and
377 delay vegetation recovery relative to fire alone (Lewis et al., 2023, 2012; Robichaud et al.,
378 2020). These interactions highlight the need for monitoring frameworks that explicitly account
379 for disturbance sequencing and pathway interactions.

380 4.2 Disturbance-threat-indicator pathways

381 A useful way to interpret how RS is being used within the forest soil context is to break down the
382 disturbance-threat-indicator pathway that links an initiating event to the soil threat of concern
383 and to the indicator(s) that RS can plausibly detect. This framing helps explain why some threats
384 are well represented in the evidence base while others remain largely invisible without ground
385 validation. To understand where sensor-based monitoring can be most effective, we can match
386 major disturbances with known soil degradation threats and associated indicators (Jordan et al.,
387 2026) and classify observability as *direct* (sensor measures the indicator itself), *proxy-based*
388 (sensor measures a correlated surface expression), or *limited* (indicator is predominantly
389 subsurface/chemical/biological and requires field validation) (Table 1). This pathway-based
390 framing is also directly relevant for indicator development in reporting contexts, where only
391 indicators with clear threat linkages and transparent observability can be operationalized
392 consistently across regions and disturbance types.



393 *4.2.1 Observability of dominant pathways*

394 Wildfire and forest harvesting practices dominate the evidence base because they generate
395 surface-expressed signals that are tractable for RS. This advantage is most pronounced for
396 stand-replacing disturbances, where canopy removal exposes soil and combustion residues. By
397 contrast, partial burns or partial cuts may not expose enough soil signal for robust RS inference.
398 After a stand-replacing fire event, canopy loss and combustion residues create clear spectral
399 signals that multispectral sensors can map efficiently over large areas. Harvesting of trees and
400 subsequent silvicultural prescriptions, produces discontinuous, fine-scale deformation (ruts,
401 berms, altered organic layer, debris piles) requiring high-resolution structural sensing to resolve.
402 This difference in signal geometry and persistence explains much of the divergence in sensor
403 choice, scale, and timing seen across the literature.

404 Wildfire can generate multiple threats to soil condition, including erosion, altered soil organic
405 carbon (SOC), biodiversity changes, and short-term nitrogen surges (Jordan et al., 2026). In
406 many cases, the resulting surface expression of burn severity produces strong, spatially coherent
407 spectral contrasts that are well captured by multispectral data (Chafer, 2008; Guindon et al.,
408 2021; Key and Benson, 2006). Short wave infrared bands (SWIR) bands are especially
409 informative because sensitivity to moisture and char improves discrimination among severity
410 classes. At finer scales, UAV multispectral data can predict composite soil burn severity more
411 robustly than single surface metrics (e.g., ash depth alone) (Beltrán-Marcos et al., 2021; Fraser et
412 al., 2017; Llorens et al., 2024). However, the timing of acquisitions is critical: detectability of
413 soil-relevant contrasts declines rapidly with regrowth and surface wetting/drying cycles, which is
414 why disturbance-proximal acquisitions anchor operational workflows (Kokaly et al., 2007;
415 Moody et al., 2013; Robichaud et al., 2007). In contrast, SOC loss, short-lived mineral-N pulses,



416 and below-ground biodiversity responses are not directly observable with RS in forested settings
417 (Whitman et al., 2020) (Table 1). SOC change can sometimes be inferred along burn-severity
418 gradients, but absolute stock losses require field sampling. Nitrogen pulses and microbial/faunal
419 shifts are field-dependent, with RS products used mainly to stratify sampling by severity and
420 connectivity (Jordan et al., 2026; Lewis et al., 2012; Llorens et al., 2024; Mallinis et al., 2009;
421 Pellegrini et al., 2021; Veraverbeke et al., 2018).

422 Harvesting operations and subsequent silvicultural prescriptions introduce soil threats primarily
423 through mechanical disturbance, including compaction, rutting, alteration of the forest floor and
424 debris piles (Cambi et al., 2018; Giannetti et al., 2017; Haas et al., 2016; Marra et al., 2018).
425 These processes, coupled with the removal of canopy, reduce porosity, alter infiltration, and
426 increase erosion risk (Giannetti et al., 2017; Haas et al., 2016; Marra et al., 2018; Nevalainen et
427 al., 2017; Pierzchała et al., 2016; Talbot et al., 2018)(Jordan et al., 2026). Unlike wildfire,
428 harvesting footprints are discontinuous and fine scale, with most severe impacts often confined
429 to skid trails, landings, and haul roads, but less severe, but broader scale impacts occurring
430 across the cut block. Soil-surface deformation and displacement (e.g., rut depth/width, berms,
431 trail/landing footprints, microrelief) are directly observable with high-resolution structural
432 sensing, notably UAV photogrammetry/ Structure-from-Motion (SfM) (e.g., Haas et al., 2016;
433 Marra et al., 2018; Nevalainen et al., 2017; Pierzchała et al., 2016), and airborne or portable
434 LiDAR (e.g., Giannetti et al., 2017; Melendy et al., 2018; Mohieddinne et al., 2023). Some
435 common indicators of post-harvest soil degradation, most notably compaction, are only
436 proxy-observable with RS. For example, compaction can be inferred from rut geometry, surface
437 roughness, or ponding patterns. Some of the most consequential subsurface indicators of
438 harvesting damage to soil remain limited to field validation: bulk density, porosity, and hydraulic



439 conductivity cannot be retrieved remotely and require in situ testing (Cambi et al., 2018;
440 Giannetti et al., 2017; Marra et al., 2018). In practice, post-harvesting assessments use
441 high-resolution disturbance maps to stratify and target the field work that quantifies subsurface
442 condition (Talbot and Astrup, 2021).

443 *4.2.2 How threat pathways appear in the evidence base*

444 The pathway logic developed in this section aligns closely with what the evidence map reports:
445 disturbances most frequently studied are those linked to soil indicators with strong surface
446 expression and high remote-sensing observability (see Table 1). In post-wildfire assessments,
447 burn severity indices dominate, followed by measures of char/ash and vegetation or substrate
448 cover (e.g., NDVI, NBR). Methodologically, wildfire studies overwhelmingly rely on optical
449 multispectral satellite data (especially Landsat and Sentinel-2) because SWIR/NIR sensitivity to
450 ash, char, exposed soil and vegetation loss enables robust, landscape-scale mapping across long
451 time series and diverse biomes (e.g., Beltrán-Marcos et al., 2023; Guindon et al., 2021; Kadakci
452 Koca, 2023). Seasonal spectral trajectories derived from dense Landsat time series have similarly
453 been shown to capture post-fire shifts in NDVI and NBR phenology, supporting the use of
454 temporal metrics as indicators of disturbance and recovery (Rose and Nagle, 2021).

455 By contrast, harvesting produces discontinuous, fine-scale surface deformation that requires
456 structural sensors and high-resolution products. As such, harvesting studies employ UAV-based
457 SfM photogrammetry (e.g., Haas et al., 2016; Marra et al., 2018; Nevalainen et al., 2017;
458 Pierzchała et al., 2016) and LiDAR (e.g., Giannetti et al., 2017; Melendy et al., 2018;
459 Mohieddinne et al., 2023) to reconstruct rut geometry and surface disturbance in three
460 dimensions. Other significant impacts of harvesting traffic, such as subsurface compaction,
461 appear in the evidence base primarily through paired designs where sensor-derived disturbance



462 maps are used to stratify sampling and interpret field measurements (e.g., Cambi et al., 2018;

463 Dubé and Berch, 2013).

464



Table 1 Threat-indicator observability matrix linking key forest soil degradation threats and associated indicators to remote-sensing observability (direct, proxy-based, or limited) and their level of representation in the mapped evidence base. “Direct” indicates indicators commonly measurable as surface expressions, “proxy-based” indicates reliance on correlated disturbance signals, and “limited” indicates indicators generally requiring field/laboratory validation.

Threat (from Jordan et al 2026)	Indicator(s) (from Jordan et al. 2026)	RS observability	Representation in evidence base
Soil erosion	Bare soil exposure, ground cover loss	Direct – optical/SWIR, UAV/airborne multispectral, cover fractions	Well represented
	Presence of rills, channels, gullies	Direct – site scale, high resolution SfM/LiDAR surface models	Well represented
	Sediment yield/delivery	Limited – requires hydrologic monitoring; RS can support proxy factors like cover/shape	Somewhat represented
Soil organic carbon change (SOC)	SOC concentration/stock	Proxy-based – spectral/statical models; strongest where soil is exposed or canopy is sparse	Somewhat represented
	Char/combustion residues	Proxy-based – mapped via burn severity	Somewhat represented
Soil biodiversity change	Microbial biomass, enzymatic activity	Limited – lab-based, RS can only support stratification by severity/cover/temperature	Not represented
	Soil fauna indicators	Limited – field-based, RS can only support stratification by severity/cover/temperature	Not represented



Nutrient mismanagement	Total/available nutrients (e.g., N, P, base cations)	Proxy-based – spectral models; RS can add disturbance context	Somewhat represented
	pH, cation exchange capacity	Limited – field/lab-based, RS can only support stratification by severity/cover/temperature	Somewhat represented
Salt accumulation	Electrical conductivity, salinity	Limited – context specific; field chemistry required	Not represented
Soil pollution	Presence of contaminants (e.g., metals, hydrocarbons)	Limited – context specific; field chemistry required	Not represented
Soil sealing and urbanization	Impervious surface	Direct – classification possible with RS, but conceptually outside forest post-disturbance pathways	Not represented
Physical degradation	Surface deformation	Direct – fine-scale UAV SfM/LiDAR DEM differencing	Well represented
	Compaction (bulk density, penetration resistance)	Proxy-based – RS can infer from rut geometry / roughness / ponding, field confirmation needed	Well represented
	Hydraulic conductivity/infiltration capacity	Limited – RS can stratify based on deformation / ponding patterns, but field instrumentation needed	Somewhat represented



466 *4.2.3 Pathways with limited observability and threat–indicator mismatch*

467 Not all disturbance-threat pathways produce surface expressions that are stable or diagnostic
468 enough for direct observation with RS. As a result, pathways dominated by subsurface physical
469 change or chemical and biological alteration remain under-represented in the evidence base, even
470 when they are highly relevant to long-term soil functioning and site productivity. This reflects a
471 fundamental observability constraint, not a lack of ecological importance. Across disturbances,
472 indicators such as bulk density, porosity, hydraulic conductivity, nutrient availability, pH,
473 salinity, and soil biodiversity metrics generally require field or laboratory measurement
474 (Table 1). Where RS contributes, it does so indirectly by mapping correlated surface conditions
475 (e.g., disturbance footprint, vegetation loss, surface deformation, moisture regime) that co-vary
476 with subsurface processes. These proxy approaches support spatial stratification and hypothesis
477 testing but typically require local calibration and repeated field validation, limiting transferability
478 across forest types and regions (Table 1).

479 This constraint helps explain why insect outbreaks, windthrow, and mining are sparsely
480 represented relative to wildfire and harvesting. For insect outbreaks, RS readily maps defoliation
481 severity, yet the soil pathways of interest (nutrient cycling shifts, leaching signals, microbial
482 responses) are largely field-dependent, making RS most defensible as disturbance context rather
483 than as a soil indicator (e.g., coupling Landsat-derived defoliation with soil/solution N, Conrad-
484 Rooney et al., 2020). In windthrow, pit-mound microtopography is detectable from
485 high-resolution 3D data, but observability windows are short and performance depends on data
486 quality and point-cloud classification, limiting routine operations (e.g., Godziek, 2024). In
487 mining contexts, dominant indicators are often chemical or subsurface (contamination, salinity,



488 acidity), placing them largely outside current forest-focused RS workflows (e.g., Lee et al.,
489 2023).

490 A recurring operational issue is threat-indicator mismatch, where commonly mapped RS
491 indicators do not directly represent the soil threat of management concern. In wildfire contexts,
492 widely used severity products often track vegetation change more strongly than soil impacts
493 unless explicitly calibrated to soil-focused severity frameworks and validated against ground
494 indicators. In harvesting, high-resolution 3D products derived from UAV SfM photogrammetry
495 and airborne/terrestrial LiDAR can map where disturbance occurred (e.g., rut geometry,
496 displaced material), typically via DEM/DTM differencing or point-cloud change detection.
497 However, subsurface compaction and hydraulic impairment must be inferred and confirmed
498 through field measurements (e.g., Kim et al., 2025; Marra et al., 2018; Nevalainen et al., 2017).
499 The practical remedy is to make the threat-indicator link explicit: state the threat, identify what is
500 directly observed versus inferred, justify any proxy relationship and its limits, and treat RS
501 products as stratification/decision-support layers when targets are subsurface or biogeochemical.

502 Overall, RS is most reliable when degradation is persistently surface-expressed and least reliable
503 when signals are ephemeral or subsurface. Accordingly, designs should prioritize
504 disturbance-proximal acquisitions for short-lived surface signals; select SWIR-inclusive optics
505 (wildfire) or high-resolution structural sensing (harvesting) matched to the pathway; and pair RS
506 with targeted field validation wherever indicators are proxy-based or calibration-sensitive.

507 4.3 Constraints on operational soil monitoring in forest landscapes

508 Even when disturbance-threat-indicator pathways are clear, operational soil monitoring in forests
509 is limited by canopy/understory occlusion, moisture dynamics and seasonality, and



510 topography/illumination, which together raise uncertainty and validation burden. In contrast to
511 agricultural systems, where frequent bare-soil exposure accelerates method standardization,
512 forests offer fewer, shorter observation windows, making inference more opportunistic and
513 disturbance-contingent.

514 *4.3.1 Canopy and understory occlusion*

515 In optical systems, overstory/understory signals frequently dominate pixel reflectance, so
516 satellite-derived indices often correlate more strongly with vegetation and surface cover than
517 with soil processes occurring beneath the canopy (Fernández-Guisuraga et al., 2022; Hudak et
518 al., 2007). This same constraint extends to high-resolution structural approaches: UAV SfM
519 point clouds can concentrate returns in the upper canopy and undergrowth, resulting in a ground
520 model that is too sparse or constrained in densely vegetated areas (Nevalainen et al., 2017). Even
521 when canopy gaps exist (e.g., along trails), discontinuities and partial exposure can complicate
522 detection and often require workflow adaptations such as low-altitude flights or denser image
523 overlap to improve ground model continuity (Nevalainen et al., 2017; Talbot and Astrup, 2021).

524 *4.3.2 Moisture interference and seasonality*

525 Moisture is both a target variable and a major source of confounding variability. Post-fire SWIR-
526 based indices, for example, are highly sensitive to surface wetness, and fluctuations in drying or
527 rehydration can shift spectral values independently of changes in soil condition (Beltrán-Marcos
528 et al., 2021; Llorens et al., 2024). Soil moisture varies with texture, microtopography, canopy
529 interception, and recent weather, making it difficult to determine whether observed spectral or
530 structural differences reflect degradation or transient hydrological states. Seasonality amplifies
531 these challenges: snowmelt, spring saturation, and prolonged cloud cover limit the number of



532 stable observation windows, especially in boreal and temperate climates (Niemi et al., 2017).
533 Even dense satellite time series (e.g., Sentinel-2) may include gaps that preclude tightly timed
534 post-disturbance analyses (Llorens et al., 2024). As a result, operational soil monitoring requires
535 clearly defined seasonal acquisition windows, explicit handling of moisture as a covariate, and
536 the strategic incorporation of SAR data, which is less constrained by illumination and cloud
537 cover. However, SAR-based inference remains sensitive to wavelength choice and forest
538 structure, leading to context-dependent performance (Fernández-Guisuraga et al., 2022).

539 *4.3.3 Topography and illumination effects*

540 Slope and aspect introduce systematic reflectance differences due to variable illumination
541 geometry, shadows, and bidirectional reflectance effects. These influences can bias optical
542 metrics and create apparent gradients in soil exposure, burn severity, or vegetation recovery that
543 are unrelated to actual soil processes (Kadakci Koca, 2023; Quintano et al., 2019). In post-fire
544 mapping, for example, severity estimations may vary with topographic position rather than with
545 combustion intensity if terrain effects are not corrected. These issues are magnified in UAV
546 imagery, where fine-scale illumination variability, deep shadows, and occlusions can degrade
547 orthomosaics and distort surface-model change detection (Marra et al., 2021). Structural data
548 also face limitations: LiDAR point-cloud classification can misidentify understory vegetation or
549 debris as ground surface in steep or complex terrain (Nevalainen et al., 2017). Effective
550 operational workflows therefore require robust topographic correction, careful shadow
551 management, and illumination-aware acquisition planning to distinguish true soil-surface change
552 from geometric artifacts.



553 *4.3.4 Technology implementation time lags*

554 Together, canopy occlusion, moisture variability, and topographic complexity contribute to a
555 broader “implementation lag” for operational, soil-focused RS in forests. While agricultural
556 applications have benefited from extensive bare-soil periods, stable phenology, and consistent
557 observation conditions that support rapid sensor and index development, forest environments
558 provide limited and often disturbance-dependent windows in which soil conditions can be
559 observed. Rapid vegetation regrowth, seasonal wetness, and strong dependence on proxy
560 indicators slow the development and uptake of standardized soil-monitoring products (Fassnacht
561 et al., 2024). Consequently, forest applications remain dominated by site-specific studies,
562 experimental methods, and nested designs that use broad-scale optical screening to direct
563 targeted UAV/LiDAR surveys (e.g., Puliti et al., 2018; Talbot et al., 2018). High-resolution
564 structural workflows (e.g., DEM differencing) also require rigorous reporting of vertical
565 uncertainty and limits of detection to separate true soil change from noise (Nevalainen et al.,
566 2017; Rengers et al., 2016). As a result, RS continues to function best as a complementary
567 component of integrated soil-monitoring systems rather than a stand-alone replacement for field
568 measurement.

569 **4.4 Scale and timing trade-offs in post-disturbance soil monitoring**

570 The value of RS application depends not only on whether indicators are observable, but on
571 where and when they can be captured relative to management objectives. Study areas in the
572 evidence base span hundreds of square metres to hundreds of thousands of hectares, with designs
573 clustering around the spatial footprint of the threat (e.g., broad-footprint erosion vs.



574 narrow-footprint rutting) and the temporal window during which surface expressions remain
575 detectable.

576 *4.4.1 Short-term detection vs long-term recovery tracking*

577 Short-term, post-disturbance mapping leverages strong but transient surface contrasts, such as
578 ash/char deposition, exposed mineral soil, and abrupt vegetation loss after fire, or cleat surface
579 deformation following traffic, making disturbance-proximal acquisitions especially effective for
580 triage, erosion-risk screening, and early stabilization planning (e.g., Burned area mapping
581 workflows based on NBR/dNBR) (Chafer, 2008; Perbet et al., 2025; White, 2024). This design
582 logic is reflected in our synthesis: acquisition years frequently coincide with disturbance and
583 sampling windows, reflecting the operational need to capture short-lived surface expressions
584 while they remain detectable. It is important to note, however, that because timing in Figure 7
585 was compiled at annual resolution, cases plotted as “same-year” may represent imagery acquired
586 weeks to months pre- and post-event. This granularity is sufficient to show the strong emphasis
587 on disturbance-proximal observation but does not resolve month-scale dynamics, which matters
588 where signals attenuate quickly. Spectrally, inclusion of SWIR bands improves discrimination
589 among post-fire severity classes when moisture and char fractions are changing rapidly. At finer
590 scales, UAV multispectral data can predict composite soil burn severity more robustly than
591 single surface metrics, which further motivates early acquisitions before signal attenuation
592 (Beltrán-Marcos et al., 2021; Llorens et al., 2024).

593 By contrast, assessing long-term recovery requires observation strategies that extend beyond the
594 period of maximum detectability. As vegetation regrows, litter and debris accumulate, and
595 surface moisture regimes normalize, surface-expressed indicators weaken, and the soil attributes
596 of greatest long-term significance (e.g., hydraulic function, SOC stability, and broader



597 biogeochemical trajectories) become increasingly field-dependent (Lewis et al., 2017;
598 Mohieddinne et al., 2019). In practice, this pushes monitoring toward a two-tier approach: (i)
599 early RS to map disturbance footprints and surface indicators for screening and stratification,
600 followed by (ii) targeted, field-anchored campaigns and repeated acquisitions to track recovery
601 processes that RS cannot directly measure with confidence.

602 *4.4.2 Broad-scale screening vs site-scale diagnosis*

603 Spatial scale choices in the evidence base also highlight a contrast between broad-scale screening
604 and site-scale diagnosis. The evidence base shows that broad-footprint outcomes, particularly
605 soil burn severity and post-fire erosion, most often pair with multispectral satellite systems. This
606 is consistent with previous studies demonstrating that these systems offer standardized,
607 repeatable coverage suitable for landscape-to-regional mapping (Guindon et al., 2021; Perbet et
608 al., 2025). In contrast, the evidence base suggests that narrow and discontinuous mechanically
609 induced outcomes, such as rutting, displacement, and compaction proxies along skid trails and at
610 landings, were consistently mapped using very-high-resolution structural sensing. This reliance
611 on UAV/SfM photogrammetry and LiDAR for fine-scale assessments is also supported by prior
612 studies (e.g., Pierzchała et al., 2014; Talbot et al., 2018; Venanzi et al., 2023). This produces a
613 practical trade-off: coarse-resolution approaches maximize coverage and comparability but offer
614 limited mechanistic specificity, whereas fine-resolution approaches deliver diagnostic detail at
615 the expense of coverage efficiency and cross-site uniformity (Talbot and Astrup, 2021).

616 To bridge these scales, many applications adopt nested designs: use regional satellite screening
617 to identify and prioritize high-risk areas, then deploy targeted UAV/LiDAR diagnostics to
618 quantify mechanisms (e.g., rut depth/width, displaced volumes, microtopography) where
619 management action is most needed (e.g., Latterini et al., 2020; Talbot et al., 2018). This



620 combination preserves regional consistency for decision-making while capturing the site-scale
621 resolution required for mitigation and adaptive planning (Kokaly et al., 2007; Pierzchała et al.,
622 2014).

623 It is important to note that most studies used multi-sensor and/or multi-scale designs, making it
624 difficult to assign a single spatial extent to a specific sensor or platform. Publications typically
625 report a single overall study area (e.g., an entire fire footprint) alongside plot sizes for validation,
626 without specifying how coverage was divided across methods; sensor-specific footprints are thus
627 often implicit.

628 Overall, the trade-off between broad-scale coverage and site-scale diagnostic resolution is well
629 documented: greater mechanistic specificity entails reduced coverage efficiency (higher per-site
630 effort and cost) and limited generalization (Puliti et al., 2018), a pattern also evident in national
631 Landsat time-series monitoring where synoptic consistency is achieved at the expense of
632 fine-scale diagnostic detail. Nested, multiresolution designs therefore remain essential for linking
633 coarse-scale screening with the fine-scale diagnostics needed to interpret underlying
634 mechanisms, especially when standardized satellite time-series products provide consistent but
635 non-mechanistic baselines (White et al., 2017).

636 *4.4.3 Validation requirements and uncertainty*

637 Validation requirements increase as monitoring products are transferred across broader spatial
638 extents or rely on indirect indicators. In post-wildfire contexts, this is evident in how severity
639 products often track vegetation change more directly than soil effects, making explicit calibration
640 to soil-burn-severity frameworks and field indicators essential (Beltrán-Marcos et al., 2021;
641 Chafer, 2008; Marcos et al., 2018). Similar constraints arise when optical indices are used to



642 infer soil properties that are only intermittently exposed; threat–indicator coherence becomes
643 increasingly context-dependent and degrades with canopy cover, moisture variability, and site
644 heterogeneity (Beltrán-Marcos et al., 2023; Kadakci Koca, 2023). For SAR-based approaches,
645 transferability is also conditional: models of post-fire soil properties can perform well, but
646 sensitivity to wavelength and forest structure reinforces the need for local calibration and explicit
647 uncertainty reporting (Fernández-Guisuraga et al., 2022).

648 For fine-scale, structurally expressed soil threats (e.g., rutting, soil displacement), uncertainty
649 often stems from measurement and processing limits (e.g., point density, vegetation masking, or
650 surface-model generation) rather than sensor physics alone. These uncertainties must be
651 validated to distinguish true change from noise. Best practice includes accounting for elevation
652 error when differencing surface models and applying a limit of detection (LoD) threshold below
653 which apparent change is discarded (Rengers et al., 2016). In forest settings, however, vegetation
654 cover reduces ground-surface capture quality, limiting the accuracy of rut and microtopography
655 measurements (Nevalainen et al., 2017; Talbot et al., 2018). Reporting vertical uncertainty and
656 the selected LoD, as well as qualifying sparse-return or understory-dense areas as lower
657 confidence, strengthens defensibility of surface-change indicators in operational contexts (Mesa-
658 Mingorance and Ariza-López, 2020).

659 *4.4.4 Proactive vs reactive monitoring: required baseline*

660 A key distinction in post-disturbance soil monitoring is whether inference relies on proactive
661 baselines (pre-event) or reactive observations (post-event only). The evidence base shows this
662 split aligns strongly with disturbance type and scale: wildfire studies overwhelmingly use
663 pre-event imagery and spectral differencing (e.g., dNBR), with explicit pre-disturbance
664 acquisitions reported almost exclusively for fire cases. This reflects the practicality of



665 long-running satellite archives that enable standardized pre/post comparisons across large areas
666 at low marginal cost (Guindon et al., 2021; Quintano et al., 2019; Whitman et al., 2020). By
667 contrast, harvesting and other site-scale disturbances seldom have comparable pre-event,
668 high-resolution baselines; studies therefore map post-event surface footprints and infer
669 subsurface condition via targeted field sampling rather than true pre/post change detection (e.g.,
670 Cambi et al., 2018; Giannetti et al., 2017).

671 Baselines matter because they (i) reduce ambiguity between disturbance effects and pre-existing
672 heterogeneity (soils, topography, vegetation) and (ii) support clearer uncertainty characterization
673 for proxy-based indicators by anchoring post-event signals to known pre-conditions. Without
674 them, post-event maps risk conflating management impacts with background variability,
675 especially where soil signals are indirect or intermittently expressed. Despite this, proactive
676 baselines are difficult to maintain in forests: canopy closure, seasonal limits on exposure, and
677 field-validation needs narrow acquisition windows and raise costs, particularly for
678 high-resolution platforms. Accordingly, the evidence supports a hybrid strategy rather than a
679 strict proactive/reactive choice: maintain coarse but repeatable baselines in priority areas (e.g.,
680 periodic LiDAR, standardized seasonal satellite composites, sentinel field plots) and pair them
681 with reactive post-disturbance mapping to triage where intensive site-scale diagnostics and field
682 campaigns add the most value (Fernández-Guisuraga et al., 2022; Robichaud et al., 2007; Talbot
683 et al., 2018).

684 4.5 Evidence gaps and research priorities

685 This evidence map reveals clear strengths in RS-based soil monitoring while also exposing
686 persistent gaps. These gaps arise from fundamental observability constraints that limit which soil



687 threats can be detected remotely, uneven biogeographical and disturbance-type representation,
688 and methodological or search-design choices that bias retrieval toward certain pathways.
689 Addressing these limitations offers opportunities to expand coverage, improve uncertainty
690 handling, and enhance the value of RS for disturbance-aware soil assessment and management.

691 *4.5.1 Coverage and representation gaps*

692 A primary gap is uneven biogeographical coverage: studies cluster in boreal and temperate
693 forests, with Mediterranean systems less frequent and tropical forests rarely captured. This
694 largely reflects differences in disturbance observability and data continuity across biomes. In
695 humid tropical forests, persistent cloud cover limits optical RS; archive analyses show many
696 regions experience months-long gaps without cloud-free Landsat/Sentinel-2 observations,
697 constraining event-timed mapping and short-interval change detection (Flores-Anderson et al.,
698 2023). Even when images are available, dense canopies and rapid regrowth shorten the detection
699 window for soil-related indicators (DeVries et al., 2015; Dupuis et al., 2020). By contrast, boreal
700 and temperate forests often present more favorable conditions for soil monitoring after
701 disturbance. Seasonal leaf-off periods, and slower vegetation recovery extend the window during
702 which soil surface conditions can be observed (Melaas et al., 2016; White, 2024).

703 Apparent sensor–biome tendencies mainly mirror dominant disturbances, not inherent sensor–
704 biome fit. Multispectral data are common in Mediterranean/temperate forests because wildfire is
705 prevalent, and optical sensors excel when canopy loss exposes spectrally distinctive ash and bare
706 mineral soil (Chafer, 2008; Veraverbeke et al., 2018). In boreal forests, harvesting dominates and
707 produces persistent structural soil features that are less spectrally distinct but well captured with
708 stereo photogrammetry and LiDAR, which directly characterize topography and disturbance



709 geometry (Talbot and Astrup, 2021; Venanzi et al., 2023). In short, sensor choice in the literature
710 tends to follow disturbance expression within each biome.

711 A parallel gap is uneven disturbance representation, with wildfire and harvesting dominating
712 relative to mining, insect outbreaks, and windthrow. As noted in 4.1, this reflects a basic
713 observational advantage: these disturbances leave clearer or more persistent soil-related signals
714 (ash/char, exposed mineral soil, ruts, surface deformation) that RS can track. A methodological
715 factor likely contributed as well: the intervention search string employed in this study
716 emphasized forestry terms (“fire/burn”, “harvest/harvesting”, “insects/disease”,
717 “windthrow/blowdown”) and omitted common extractive-sector terms (e.g., mining, extraction,
718 quarry/aggregates, tailings, reclamation). Outcome terms likewise prioritized physical/hydrologic
719 pathways (compaction, rutting, skid trails, runoff/erosion, soil moisture), biasing retrieval toward
720 fire/harvest and away from chemically framed extractive pathways (contamination, acidification,
721 salinization). The only mining study retrieved, Lee et al., 2023, is consistent with this: in a
722 post-quarry restoration context, degradation was assessed via surface-visible metrics (exposed
723 soil/rock) aligned with our inclusion criteria.

724 A final gap concerns the treatment of compound or stacked disturbances. While these
725 disturbance sequences are well represented as salvage harvesting cases in the evidence base, they
726 remain comparatively poorly understood. As discussed above, stacked sequences require careful
727 attribution across overlapping temporal signals and tighter timing/resolution to separate effects
728 (Dubé and Berch, 2013; Lewis et al., 2012). High-resolution optical and LiDAR can disentangle
729 salvage impacts under favorable conditions, but applications are inconsistent, and few studies
730 frame disturbance effects cumulatively (Giannetti et al., 2017; Lewis et al., 2012; Robichaud et
731 al., 2020). Given evidence that soil impacts are non-additive (e.g., amplifying erosion risk and



732 delaying recovery) monitoring frameworks should explicitly account for disturbance sequencing
733 and pathway interactions.

734 *4.5.2 Remote sensing as operational decision support for soil protection*

735 This review has primarily considered RS as a post-disturbance monitoring tool that uses
736 indicators to report on soil degradation. A complementary application is its use as operational
737 decision support to anticipate and mitigate avoidable soil damage through planning, routing, and
738 timing before and during forest operations. Remotely sensed terrain and wetness products (e.g.,
739 LiDAR-derived DTMs) can identify traffic-sensitive zones, optimize landings and machine
740 routes, and adapt trail layout to soil-bearing capacity (Vepakomma et al., 2023). In practice,
741 wet-area indices such as depth-to-water (DTW) and topographic wetness index (TWI) are used
742 to guide access and avoid high-risk areas, while UAV orthomosaics/point clouds assess rutting
743 post-operation for compliance and iterative improvement (Vepakomma et al., 2023). Adoption is
744 growing in Nordic and Central European contexts and is shifting from static to dynamic
745 trafficability mapping as inventories improve (Hoffmann et al., 2022). Field studies show the
746 probability of severe rutting rises as DTW decreases, supporting DTW/TWI for prevention while
747 acknowledging site-to-site variability linked to soils, traffic intensity, and weather (Heppelmann
748 et al., 2022). At broader scales, satellite-derived moisture indicators support time-varying
749 operability assessments for roads and access (Fjeld et al., 2024; Hoffmann et al., 2022), whereas
750 very-high-resolution UAV/LiDAR products quantify surface disturbance post-operation and
751 provide feedback to refine planning rules (Nevalainen et al., 2017; Pierzchała et al., 2016; Talbot
752 et al., 2018). Collectively, these results indicate that RS can reduce avoidable soil damage when
753 used proactively for risk anticipation and planning, not solely for retrospective mapping.



754 *4.5.3 Emerging technologies and methodological frontiers*

755 Recent advances in sensing physics, data fusion, and analytics are expanding what is technically
756 feasible for post-disturbance soil monitoring, particularly where conventional optical or
757 structural sensors reach their observability limits. Several emerging technologies show promise
758 for overcoming long-standing challenges related to canopy occlusion, moisture interference, and
759 subsurface detectability.

760 One important frontier is quantum sensing. Cold-atom gravity gradiometers can detect density
761 contrasts at sub-metre resolution, revealing buried voids, density anomalies, or moisture
762 differences that are invisible to conventional optical or LiDAR systems (Stray et al., 2022). Stray
763 et al. demonstrated precise detection of a buried tunnel, outperforming traditional ground-gravity
764 methods, suggesting that such sensors could eventually support identification of compaction,
765 hidden water pockets, or buried layers in forest environments (Stray et al., 2022). Looking ahead,
766 NASA's Earth Science Technology Office highlights next-generation quantum-based gravity and
767 microwave detectors as promising tools for future Earth-observation systems, potentially
768 mitigating canopy and illumination constraints that limit current RS (NASA Earth Science
769 Technology Office, 2024).

770 Concurrently, hyperspectral remote sensing is enhancing detection of soil-relevant biochemical
771 and physical properties. By capturing narrow spectral features linked to mineralogy, organic
772 matter, ash/char composition, and moisture, hyperspectral systems can improve soil-signal
773 discrimination relative to broadband multispectral data and strengthen proxy relationships for
774 soil carbon and nutrient loss when paired with field spectroscopy (Tarun Kshatriya and Thamizh
775 Vendan, 2025; Yu et al., 2020). In post-fire and harvesting contexts, integrating hyperspectral
776 data with machine learning and change detection has shown promise for isolating soil-surface



777 signals (e.g., sealing, exposed mineral soil, char fractions) from overstory effects (Tarun

778 Kshatriya and Thamizh Vendan, 2025; Yu et al., 2020).

779 A complementary frontier is AI-enabled multi-sensor fusion. Deep learning and

780 physics-informed models can integrate structural (LiDAR/SfM), spectral (optical/hyperspectral),

781 and radar (C-/L-band SAR) data streams to improve inference on soil processes beneath partial

782 canopy and across complex terrain (Essbiti et al., 2025). Soil-focused studies show that fused

783 sensor-AI systems can accurately predict moisture, salinity, and nutrient availability, and

784 translate these predictions into actionable management tools (Tarun Kshatriya and Thamizh

785 Vendan, 2025). In forest applications, such approaches could enhance rut detection under partial

786 canopy, automate erosion-feature mapping, and help separate soil-burn-severity signals from

787 overlying vegetation patterns (Essbiti et al., 2025; Howari, 2025).

788 5. Conclusion

789 This evidence map synthesizes nearly three decades of research on RS for post-disturbance soil

790 monitoring and clarifies how disturbance context, sensor choice, and indicator observability

791 shape current practice. Across biomes, RS is most effective when soil degradation generates

792 persistent surface expressions, such as post-fire exposure of mineral soil or traffic-induced

793 deformation, while subsurface physical, chemical, and biological changes remain largely beyond

794 direct detection. The disturbance-threat-indicator framework used here highlights these

795 constraints and emphasizes that RS must be aligned with the specific soil threat, spatial footprint

796 of disturbance, and the temporal window during which indicators are detectable. Several

797 cross-cutting insights emerge: (1) wildfire and harvesting dominate the evidence base because

798 they produce strong or fine-scale surface signals suited to optical or structural sensors



799 respectively, (2) scale and timing strongly influence capability: broad-scale satellite observations
800 support consistent screening, whereas site-scale diagnostics require targeted, high-resolution
801 acquisitions collected closely after disturbance, (3) RS adds the most value when paired with
802 field validation, providing spatial context for interpreting soil processes that cannot be observed
803 directly.

804 Although remote sensing enables broad-scale characterization of disturbance footprints and
805 surface-expressed soil indicators, our synthesis also highlights that observability constraints
806 fundamentally limit which indicators can be operationalized for reporting purposes. Indicators
807 tied to discontinuous, fine-scale surface deformation (e.g., rutting, displacement) or persistent
808 spectral change (e.g., burn severity) have the strongest evidence base for consistent RS
809 monitoring, whereas indicators dominated by subsurface physical, chemical, or biological
810 change remain dependent on field validation and therefore cannot yet support standardized
811 reporting without hybrid RS–field workflows. These distinctions matter because global
812 assessment frameworks such as the FAO Global Forest Resources Assessment explicitly rely on
813 transparent, repeatable, indicator-driven reporting produced with acceptable consistency,
814 uncertainty, and scalability (FAO, 2025). Thus, this evidence map clarifies not only where RS
815 provides reliable post-disturbance soil information, but also which indicators are most defensible
816 for integration into emerging national and international monitoring programs, helping to define
817 realistic pathways toward reporting-ready, disturbance-aware soil indicators.

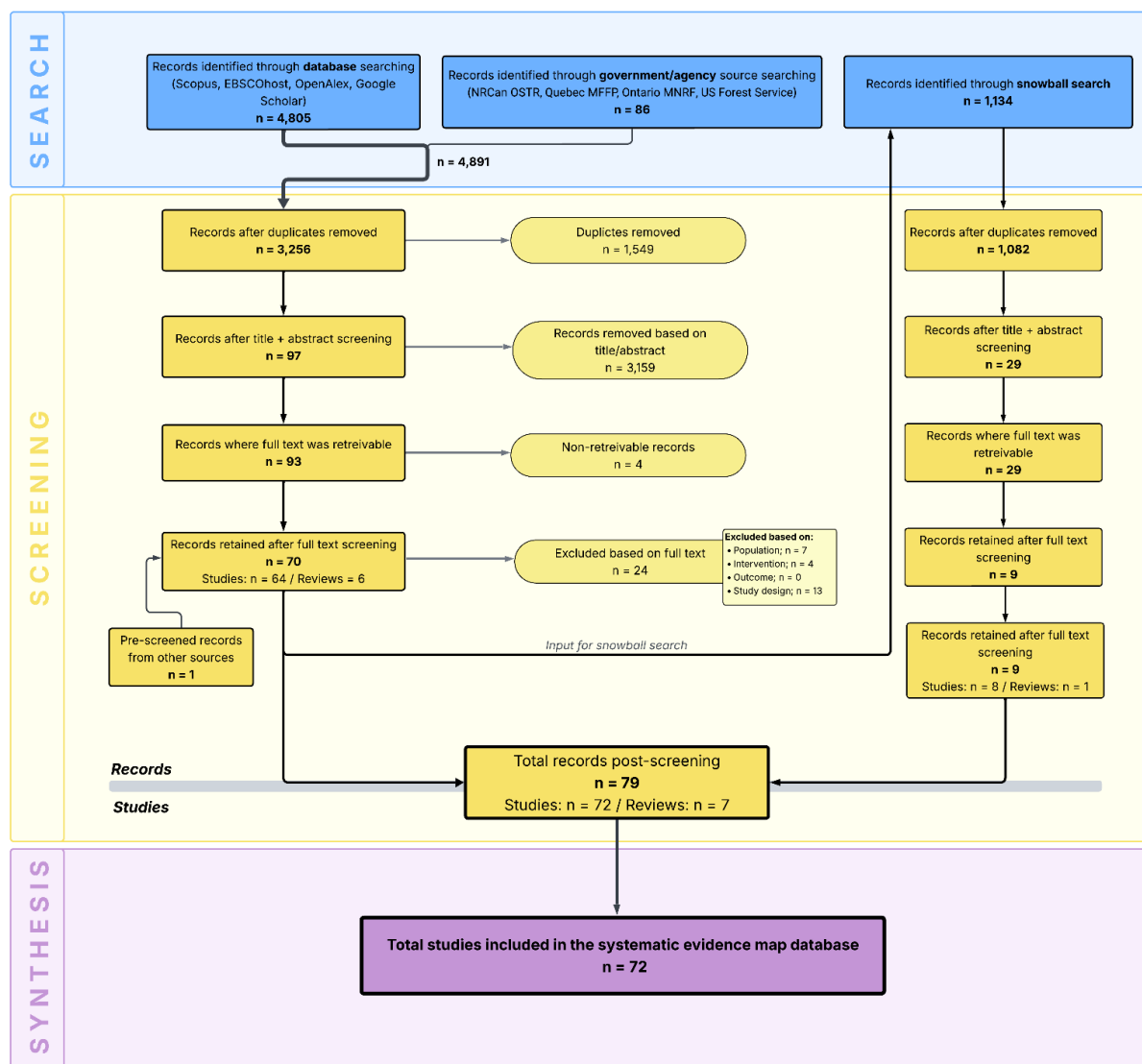
818 Overall, RS should be viewed not as a replacement for field-based assessment but as a core
819 element of integrated, multi-scale soil-monitoring systems. By clarifying strengths, limitations,
820 and evidence gaps, this synthesis provides a foundation for developing more operational,
821 disturbance-aware frameworks for protecting forest soils.



822 6. Appendix

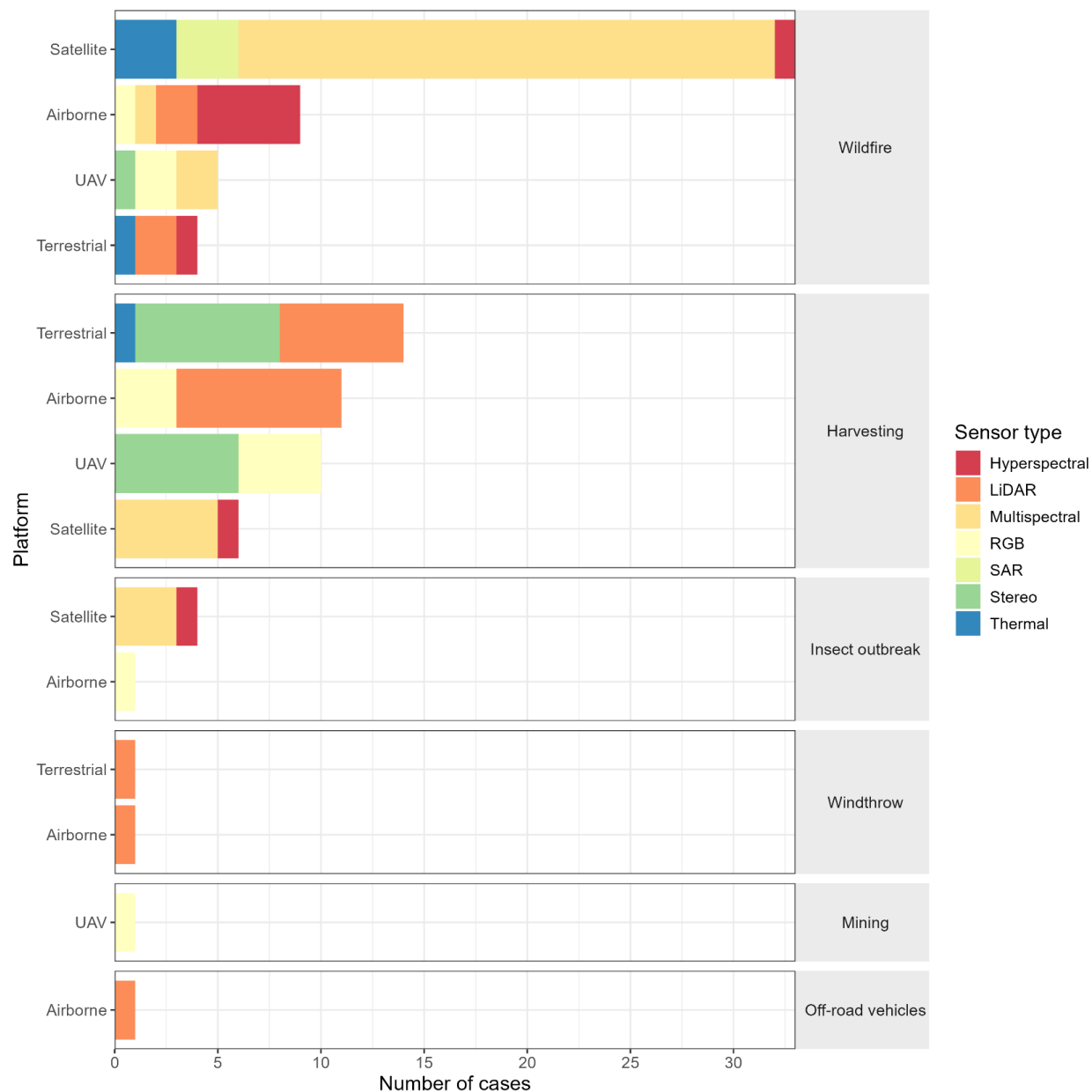
823

824 **Figure A1.** ROSES-style diagram of the article screening process for this knowledge map. Inspired by
825 template from Haddaway et al. (2018).



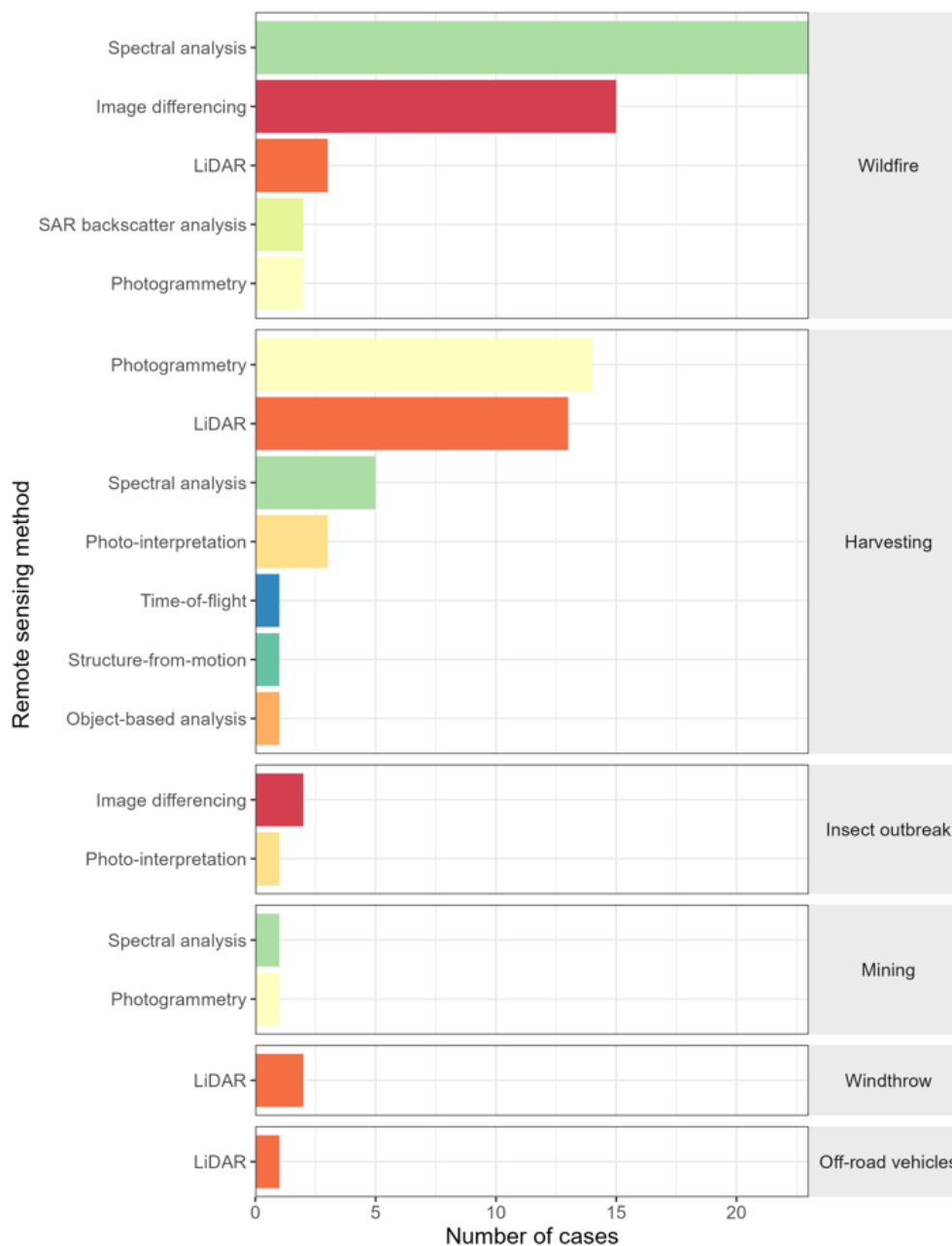


826 **Figure A2.** Number of cases of each sensor type use across RS platform types, separated by disturbance
 827 type. Note that a single study could report the use of more than one platform type, sensor type, or
 828 disturbance type, thus each combination of platform, sensor type, and disturbance type is counted as one
 829 “case” (91 cases across 72 studies).





830 **Figure A3.** Number of cases of each RS method used by disturbance type. Note that a single study could
 831 report more than one RS method or disturbance type, thus each combination of method and disturbance
 832 type is counted as one “case” (91 cases across 72 studies).



833



834 **Table A1.** Search strings used to target population, intervention, outcome, and method components of
 835 remote sensing (RS) studies that monitor forest soil degradation. The search strings include wildcards (*)
 836 and, in order of precedence, the Boolean operators NOT, AND, and OR. The strings for each of the four
 837 study components are joined with a Boolean AND.

Study component	Search string
Population <i>Target studies that focus on forest soils</i>	forest* AND soil* NOT crop* OR agri*
Intervention (Source of impacts) <i>Target studies that identify the sources of forest soil disturbances</i>	harvesting OR cut* OR clearcut* OR clear-cut* OR cutblock* OR timber OR salvage OR forestry OR “wood extraction” OR harvest OR “select* cut*” OR “select* log*” OR silvicultur* OR high*grading OR block cut* OR blowdown OR windthrow OR windsnap OR insect* OR disease* OR pest* OR fire* OR burn*
Outcome (Impacts) <i>Target studies that monitor forest soil degradation</i>	rut* OR “wheel rut*” OR wheel-rut* OR “skid trail*” OR skidder* OR feller* OR degradation OR disturbance OR compaction OR erosion OR “vegetation recovery” OR “vegetation disturbance” OR slash OR wood*slash OR drainage OR runoff OR windrow* OR scalping OR slumping OR nutrient* OR moisture
Method <i>Target studies that employ RS tools to monitor forest soil degradation</i>	“remote sensing” OR “Earth observation” OR satellite OR image* OR drone OR uav OR unmanned aerial vehicle OR aerial OR photogrammetr* OR stereoscop* OR lidar OR optical OR radar OR sensor OR *spectral OR ndvi OR “vegetation index” OR nbr OR “normali*ed burn ratio” OR dem OR “digital elevation model”

838



839 **Table A2.** Broad categories for soil degradation indicators, including definitions and included terms.

Category	Definition	Included terms
Vegetation/substrate measurements	Vegetation or substrate cover removal, abundance, or change.	Vegetation cover; canopy cover; canopy cover change; canopy height; vegetative biomass estimates; green tree retention; defoliation; defoliation index; exposed mineral soil, exposed soil and rock cover; landcover; soil type cover estimates; presence of dead wood; wood debris volume; litter depth; duff depth; depth of surface organic layer; organic soil depth; soil disturbance classification index
Spectral indices	Mathematical combinations of reflectance values from specific spectral bands used to highlight surface properties or changes in the landscape.	NDVI; NBR; RGB indices; spectral indices, disturbance index
Burn severity indices	Standardized metrics, classification systems, and RS-derived algorithms used to quantify the ecological and physical impacts of fire on vegetation and soil, and the degree of change caused by fire.	Burn severity index, composite burn severity index; composite burn index; burn severity; burn severity classes; burned area reflectance classification; fire severity index; soil burn severity; soil burn severity index
Char/ash measurements	Field- or image-based indicators that quantify or describe the presence, extent, and characteristics of burned organic material and combustion residues on the soil surface and vegetation.	Fractional/field/surface cover estimates; scorched vegetation; char depth; soil char depth; scorch depth; ash cover
Hydrologic measurements	Quantitative or qualitative assessments of water-related	Soil moisture; soil moisture content; soil water content; soil wetness; soil



	soil properties that influence infiltration, retention, and movement of water in post-fire environments.	water repellency; water drop penetration time; duff moisture content; mini-disk infiltrometer rate
Soil physical property measurements	Quantitative or qualitative assessments of the structural and mechanical characteristics of soil that influence its behavior under natural and disturbed conditions.	Bulk density; soil bulk density; soil density; soil porosity; soil compaction depth; soil penetration resistance; cone penetration resistance; penetration resistance; soil penetrability; soil resistance; soil physical properties; soil biophysical properties
Soil biochemical property measurements	Assessments of the biochemical composition and nutrient status of soil and vegetation.	Soil organic carbon; soil organic carbon content; soil carbon content; soil phosphorus content; foliar N measurements; soil pH; soil nitrogen content
Soil surface deformation/displacement measurements	Quantitative or observational assessments of physical changes in the soil surface caused by mechanical disturbance	Soil displacement; soil/volume displacement; soil volume displacement; changes in soil volume; estimated bulge volume; bulge height; depression volume; root plate volume; ground surface changes; rut depth; rut severity; rut severity index; rut volume; estimated rut volume
Road/traffic footprint measurements	Spatial and observational metrics that capture the physical presence, extent, and impact of roads, trails, and vehicle tracks on the landscape.	Road width; skid trail width measurements; spatial extent of roads and trails; presence of roadside disturbances; presence of tracks; visual track detection
Erosion and sediment measurements	Qualitative and quantitative indicators of soil loss, sediment transport, and geomorphic changes.	Presence of visual erosion; erosion severity classes; sediment yield estimates; runoff sediment volume; channel downcutting; scarp identification



Topographic measurements	Spatial data and derived metrics that describe the elevation, shape, and variability of the land surface.	Digital elevation model (DEM); digital terrain model (DTM); terrain surface modelling; slope; topographic variations; elevations change; elevation changes; change in elevation; surface roughness
Thermal measurements	Radiometric assessments of surface temperature and thermal properties, typically derived from thermal infrared (TIR) sensors	Emissivity

840

841 Code and Data Availability

842 All code and data associated with the work reported in this paper can be accessed on Zenodo:

843 <https://doi.org/10.5281/zenodo.19225706>.

844 Author contributions

845 **Maisy Roach-Krajewski**: Data curation, Investigation, Formal analysis, Methodology,
846 Visualization, Writing – Original draft. **Xavier Giroux-Bougard**: Conceptualization, Data
847 curation, Investigation, Formal analysis, Methodology, Writing – Original draft. **David Paré**:
848 Conceptualization, Funding acquisition, Writing – Review and editing. **Catlan Dallaire**:
849 Writing – Review and editing. **Luc Guindon**: Writing – Review and editing. **Florian Jordan**:
850 Writing – Review and editing. **Charlotte Norris**: Funding acquisition, Writing – Review and
851 editing. **Kara Webster**: Funding acquisition, Writing – Review and editing. **Jérôme Laganière**:
852 Conceptualization, Funding acquisition, Project administration, Supervision, Writing – Review
853 and editing.



854 Declaration of Competing Interest

855 The authors declare that they have no known competing financial interests or personal
856 relationships that could have appeared to influence the work reported in this paper.

857 Acknowledgements

858 The authors would like to thank Aicha Hezit for her contribution to the data extraction for this
859 evidence map, as well as all members of the forests soil degradation team for their valuable input
860 and constructive feedback. We would also like to acknowledge the researchers who have put
861 immeasurable time and resources into advancing this field of study. Without your work, the
862 compilation of this evidence map would not be possible.

863 Declaration of generative AI and AI-assisted technologies in the writing process: during the
864 preparation of this work the authors used Microsoft Copilot to help condense sections of the text
865 in late-stage reviewing. After using this tool, the authors reviewed and edited the content as
866 needed and takes full responsibility for the content of the published article.

867 Financial support

868 This work was funded by the Forest Systems Information and Technology Enhancement
869 (ForSITE) program of the Canadian Forest Service.



870 References

- 871 Agbeshie, A.A., Abugre, S., Atta-Darkwa, T., Awuah, R., 2022. A review of the effects of forest
872 fire on soil properties. *J. For. Res.* 33, 1419–1441. [https://doi.org/10.1007/s11676-022-](https://doi.org/10.1007/s11676-022-01475-4)
873 [01475-4](https://doi.org/10.1007/s11676-022-01475-4)
- 874 Beltrán-Marcos, D., Suárez-Seoane, S., Fernández-Guisuraga, J.M., Fernández-García, V.,
875 Marcos, E., Calvo, L., 2023. Relevance of UAV and Sentinel-2 data fusion for estimating
876 topsoil organic carbon after forest fire. *Geoderma* 430, 116290.
877 <https://doi.org/10.1016/j.geoderma.2022.116290>
- 878 Beltrán-Marcos, D., Suárez-Seoane, S., Fernández-Guisuraga, J.M., Fernández-García, V., Pinto,
879 R., García-Llamas, P., Calvo, L., 2021. Mapping soil burn severity at very high spatial
880 resolution from unmanned aerial vehicles. *Forests* 12, 179.
881 <https://doi.org/10.3390/f12020179>
- 882 Bhatnagar, S., Puliti, S., Talbot, B., Heppelmann, J.B., Breidenbach, J., Astrup, R., 2022.
883 Mapping wheel-ruts from timber harvesting operations using deep learning techniques in
884 drone imagery. *Forestry: An International Journal of Forest Research* cpac023.
885 <https://doi.org/10.1093/forestry/cpac023>
- 886 Bonan, G.B., 2008. Forests and Climate Change: Forcings, Feedbacks, and the Climate Benefits
887 of Forests. *Science* 320, 1444–1449. <https://doi.org/10.1126/science.1155121>
- 888 Borsah, A.A., Nazeer, M., Wong, M.S., 2023. LIDAR-Based Forest Biomass Remote Sensing: A
889 Review of Metrics, Methods, and Assessment Criteria for the Selection of Allometric
890 Equations. *Forests* 14, 2095. <https://doi.org/10.3390/f14102095>



- 891 Bowd, E.J., Banks, S.C., Strong, C.L., Lindenmayer, D.B., 2019. Long-term impacts of wildfire
892 and logging on forest soils. *Nature Geosci* 12, 113–118. [https://doi.org/10.1038/s41561-](https://doi.org/10.1038/s41561-018-0294-2)
893 [018-0294-2](https://doi.org/10.1038/s41561-018-0294-2)
- 894 Brown, K.J., Metsaranta, J., Paré, D., Perrakis, D.D., Van Der Kamp, D., Webster, K.L.,
895 Whitman, E., Arsenault, A., Dranga, S., Harvey, J.E. and Laganière, J., 2026. Examining
896 post-fire environmental change and succession in Canada. *Environmental Reviews*, (ja).
897 <https://doi.org/10.1139/er-2025-0224>
- 898 Bryan J., 2025. googlesheets4: Access Google Sheets using the Sheets API V4. R package
899 version 1.1.2, <https://googlesheets4.tidyverse.org>
- 900 Cambi, M., Certini, G., Neri, F., Marchi, E., 2015. The impact of heavy traffic on forest soils: A
901 review. *Forest Ecology and Management* 338, 124–138.
902 <https://doi.org/10.1016/j.foreco.2014.11.022>
- 903 Cambi, M., Giannetti, F., Bottalico, F., Travaglini, D., Nordfjell, T., Chirici, G., Marchi, E.,
904 2018. Estimating machine impact on strip roads via close-range photogrammetry and soil
905 parameters: A case study in central Italy. *iForest* 11, 148–154.
906 <https://doi.org/10.3832/ifor2590-010>
- 907 Chafer, C.J., 2008. A comparison of fire severity measures: An Australian example and
908 implications for predicting major areas of soil erosion. *CATENA* 74, 235–245.
909 <https://doi.org/10.1016/j.catena.2007.12.005>
- 910 Chen, Y., Morton, D.C., Randerson, J.T., 2024. Remote sensing for wildfire monitoring: Insights
911 into burned area, emissions, and fire dynamics. *One Earth* 7, 1022–1028.
912 <https://doi.org/10.1016/j.oneear.2024.05.014>



- 913 Collaboration for Environmental Evidence, 2022. Guidelines and Standards for Evidence
914 synthesis in Environmental Management, Version 5.1.
- 915 Conrad-Rooney, E., Barker Plotkin, A., Pasquarella, V.J., Elkinton, J., Chandler, J.L., Matthes,
916 J.H., 2020. Defoliation severity is positively related to soil solution nitrogen availability
917 and negatively related to soil nitrogen concentrations following a multi-year invasive
918 insect irruption. *AoB PLANTS* 12, plaa059. <https://doi.org/10.1093/aobpla/plaa059>
- 919 Cook, C.N., Nichols, S.J., Webb, J.A., Fuller, R.A., Richards, R.M., 2017. Simplifying the
920 selection of evidence synthesis methods to inform environmental decisions: A guide for
921 decision makers and scientists. *Biological Conservation* 213, 135–145.
922 <https://doi.org/10.1016/j.biocon.2017.07.004>
- 923 DeArmond, D., Ferraz, J.B.S., Higuchi, N., 2021. Natural recovery of skid trails: a review. *Can.*
924 *J. For. Res.* 51, 948–961. <https://doi.org/10.1139/cjfr-2020-0419>
- 925 Delgado-Baquerizo, M., Eldridge, D.J., Liu, Y.-R., Liu, Z.-W., Coleine, C., Trivedi, P., 2025.
926 Soil biodiversity and function under global change. *PLoS Biol* 23, e3003093.
927 <https://doi.org/10.1371/journal.pbio.3003093>
- 928 DeVries, B., Verbesselt, J., Kooistra, L., Herold, M., 2015. Robust monitoring of small-scale
929 forest disturbances in a tropical montane forest using Landsat time series. *Remote*
930 *Sensing of Environment* 161, 107–121. <https://doi.org/10.1016/j.rse.2015.02.012>
- 931 Dinerstein, E., Olson, D., Joshi, A., Vynne, C., Burgess, N.D., Wikramanayake, E., Hahn, N.,
932 Palminteri, S., Hedao, P., Noss, R., Hansen, M., Locke, H., Ellis, E.C., Jones, B., Barber,
933 C.V., Hayes, R., Kormos, C., Martin, V., Crist, E., Sechrest, W., Price, L., Baillie, J.E.M.,
934 Weeden, D., Suckling, K., Davis, C., Sizer, N., Moore, R., Thau, D., Birch, T., Potapov,
935 P., Turubanova, S., Tyukavina, A., De Souza, N., Pintea, L., Brito, J.C., Llewellyn, O.A.,



- 936 Miller, A.G., Patzelt, A., Ghazanfar, S.A., Timberlake, J., Klöser, H., Shennan-Farpón,
937 Y., Kindt, R., Lillesø, J.-P.B., Van Breugel, P., Graudal, L., Voge, M., Al-Shammari,
938 K.F., Saleem, M., 2017. An ecoregion-based approach to protecting half the terrestrial
939 realm. *BioScience* 67, 534–545. <https://doi.org/10.1093/biosci/bix014>
- 940 Dubé, S., Berch, S., 2013. Monitoring soil disturbance on salvaged areas within the mountain
941 pine beetle infestation using digital imagery. *J. Appl. Remote Sens* 7, 073541.
942 <https://doi.org/10.1117/1.JRS.7.073541>
- 943 Dupuis, C., Lejeune, P., Michez, A., Fayolle, A., 2020. How Can Remote Sensing Help Monitor
944 Tropical Moist Forest Degradation?—A Systematic Review. *Remote Sensing* 12, 1087.
945 <https://doi.org/10.3390/rs12071087>
- 946 Essbiti, M.C., Namous, M., Krimissa, S., Elaloui, A., Hajaj, S., Mosaid, H., Ismaili, M., Hajji, S.,
947 El Atiq, J., El Kamouni, F.E., 2025. Emerging trends and future directions in remote-
948 sensing techniques and platforms for sustainable forest degradation monitoring: a review.
949 *Med. Geosc. Rev.* 7, 953–976. <https://doi.org/10.1007/s42990-025-00184-4>
- 950 FAO, 2025. Status of the World’s Soil Resources 2025. Food and Agriculture Organization of
951 the United Nations.
- 952 Fassnacht, F.E., White, J.C., Wulder, M.A., Næsset, E., 2024. Remote sensing in forestry:
953 current challenges, considerations and directions. *Forestry: An International Journal of*
954 *Forest Research* 97, 11–37. <https://doi.org/10.1093/forestry/cpad024>
- 955 Fernández-Guisuraga, J.M., Marcos, E., Suárez-Seoane, S., Calvo, L., 2022. ALOS-2 L-band
956 SAR backscatter data improves the estimation and temporal transferability of wildfire
957 effects on soil properties under different post-fire vegetation responses. *Science of The*
958 *Total Environment* 842, 156852. <https://doi.org/10.1016/j.scitotenv.2022.156852>



- 959 Fjeld, D., Persson, M., Fransson, J.E.S., Bjerketvedt, J., Bråthen, M., 2024. Modelling forest
960 road trafficability with satellite-based soil moisture variables. *International Journal of*
961 *Forest Engineering* 35, 93–104. <https://doi.org/10.1080/14942119.2023.2276628>
- 962 Flores-Anderson, A.I., Cardille, J., Azad, K., Cherrington, E., Zhang, Y., Wilson, S., 2023.
963 Spatial and Temporal Availability of Cloud-free Optical Observations in the Tropics to
964 Monitor Deforestation. *Sci Data* 10, 550. <https://doi.org/10.1038/s41597-023-02439-x>
- 965 Fraser, R., Van Der Sluijs, J., Hall, R., 2017. Calibrating Satellite-Based Indices of Burn Severity
966 from UAV-Derived Metrics of a Burned Boreal Forest in NWT, Canada. *Remote Sensing*
967 9, 279. <https://doi.org/10.3390/rs9030279>
- 968 Gao, Y., Skutsch, M., Paneque-Gálvez, J., Ghilardi, A., 2020. Remote sensing of forest
969 degradation: a review. *Environ. Res. Lett.* 15, 103001. [https://doi.org/10.1088/1748-](https://doi.org/10.1088/1748-9326/abaad7)
970 [9326/abaad7](https://doi.org/10.1088/1748-9326/abaad7)
- 971 Ge, Y., Thomasson, J.A., Sui, R., 2011. Remote sensing of soil properties in precision
972 agriculture: A review. *Front. Earth Sci.* <https://doi.org/10.1007/s11707-011-0175-0>
- 973 Giannetti, F., Chirici, G., Travaglini, D., Bottalico, F., Marchi, E., Cambi, M., 2017. Assessment
974 of soil disturbance caused by forest operations by means of portable laser scanner and
975 soil physical parameters. *Soil Science Soc of Amer J* 81, 1577–1585.
976 <https://doi.org/10.2136/sssaj2017.02.0051>
- 977 Godziek, J., 2024. Root plates of uprooted trees – Automatic detection and biotransport
978 estimation using LiDAR data and field mapping. *International Journal of Applied Earth*
979 *Observation and Geoinformation* 131, 103992. <https://doi.org/10.1016/j.jag.2024.103992>



- 980 Guindon, L., Gauthier, S., Manka, F., Parisien, M.-A., Whitman, E., Bernier, P., Beaudoin, A.,
981 Villemaire, P., Skakun, R., 2021. Trends in wildfire burn severity across Canada, 1985 to
982 2015. *Can. J. For. Res.* 51, 1230–1244. <https://doi.org/10.1139/cjfr-2020-0353>
- 983 Haas, J., Hagge Ellhöft, K., Schack-Kirchner, H., Lang, F., 2016. Using photogrammetry to
984 assess rutting caused by a forwarder—A comparison of different tires and bogie tracks.
985 *Soil and Tillage Research* 163, 14–20. <https://doi.org/10.1016/j.still.2016.04.008>
- 986 Haddaway, N., Macura, B., Whaley, P., Pullin, A., 2018. ROSES flow diagram for systematic
987 maps. Version 1.0. <https://doi.org/10.6084/M9.FIGSHARE.6085940>
- 988 Harzing, A.W., 2007. Publish or perish. Available at [https://harzing.com/resources/publish-or-](https://harzing.com/resources/publish-or-perish)
989 [perish](https://harzing.com/resources/publish-or-perish).
- 990 Heppelmann, J.B., Talbot, B., Antón Fernández, C., Astrup, R., 2022. Depth-to-water maps as
991 predictors of rut severity in fully mechanized harvesting operations. *International Journal*
992 *of Forest Engineering* 33, 108–118. <https://doi.org/10.1080/14942119.2022.2044724>
- 993 Hoffmann, S., Schönauer, M., Heppelmann, J., Asikainen, A., Cacot, E., Eberhard, B.,
994 Hasenauer, H., Ivanovs, J., Jaeger, D., Lazdins, A., Mohtashami, S., Moskalik, T.,
995 Nordfjell, T., Stereńczak, K., Talbot, B., Uusitalo, J., Vuillermoz, M., Astrup, R., 2022.
996 Trafficability Prediction Using Depth-to-Water Maps: the Status of Application in
997 Northern and Central European Forestry. *Curr Forestry Rep* 8, 55–71.
998 <https://doi.org/10.1007/s40725-021-00153-8>
- 999 Howari, F., 2025. AI–Remote Sensing for Soil Variability Mapping and Precision Agrochemical
1000 Management: A Comprehensive Review of Methods, Limitations, and Climate-Smart
1001 Applications. *Agrochemicals* 5, 1. <https://doi.org/10.3390/agrochemicals5010001>



- 1002 Hudak, A., Robichaud, P.R., Jain, T., Morgan, P., Stone, C., Clark, J., 2004. The relationship of
1003 field burn severity measures to satellite-derived Burned Area Reflectance Classification
1004 (BARC) maps. American Society of Photogrammetry and Remote Sensing Conference
1005 Proceedings.
- 1006 Hudak, A.T., Morgan, P., Bobbitt, M.J., Smith, A.M.S., Lewis, S.A., Lentile, L.B., Robichaud,
1007 P.R., Clark, J.T., McKinley, R.A., 2007. The relationship of multispectral satellite
1008 imagery to immediate fire effects. *fire ecol* 3, 64–90.
1009 <https://doi.org/10.4996/fireecology.0301064>
- 1010 Jordan, F., Paré, D., Norris, C., Webster, K., Dallaire, C., Laganière, J., 2026. Understanding
1011 forest soil degradation in Canada: current knowledge, threats and indicators - a review,
1012 *Canadian Journal of Forest Research*, submitted.
- 1013 Kadakci Koca, T., 2023. A statistical approach to site-specific thresholding for burn severity
1014 maps using bi-temporal Landsat-8 images. *Earth Sci Inform* 16, 1313–1327.
1015 <https://doi.org/10.1007/s12145-023-00980-2>
- 1016 Key, C.H., Benson, N.C., 2006. *Landscape Assessment (LA)*.
- 1017 Kim, I., Seo, J., Woo, H., Choi, B., 2025. Assessing rutting and soil compaction caused by wood
1018 extraction using traditional and remote sensing methods. *Forests* 16, 86.
1019 <https://doi.org/10.3390/fl6010086>
- 1020 Kokaly, R.F., Rockwell, B.W., Haire, S.L., King, T.V.V., 2007. Characterization of post-fire
1021 surface cover, soils, and burn severity at the Cerro Grande Fire, New Mexico, using
1022 hyperspectral and multispectral remote sensing. *Remote Sensing of Environment* 106,
1023 305–325. <https://doi.org/10.1016/j.rse.2006.08.006>



- 1024 Kubiak, K., Spiralski, M., Pompeu, J., Levavasseur, V., Wawer, R., 2024. Advances in Remote
1025 Sensing for Monitoring Soil Conditions in Forest Ecosystems: Techniques, Challenges,
1026 and Applications. *Transactions on Aerospace Research* 2024, 1–13.
1027 <https://doi.org/10.2478/tar-2024-0019>
- 1028 Latterini, F., Venanzi, R., Tocci, D., Moschetti, F., Picchio, R., 2020. Comparing accuracy of
1029 three remote sensing methods to evaluate soil impact related to forest operations, in: *The*
1030 *1st International Electronic Conference on Forests—Forests for a Better Future:*
1031 *Sustainability, Innovation, Interdisciplinarity*. Presented at the International Electronic
1032 Conference on Forests, MDPI, p. 59. <https://doi.org/10.3390/IECF2020-07954>
- 1033 Lausch, A., Erasmi, S., King, D., Magdon, P., Heurich, M., 2016. Understanding Forest Health
1034 with Remote Sensing -Part I—A Review of Spectral Traits, Processes and Remote-
1035 Sensing Characteristics. *Remote Sensing* 8, 1029. <https://doi.org/10.3390/rs8121029>
- 1036 Lee, K., Elliott, S., Tiansawat, P., 2023. Use of drone RGB imagery to quantify indicator
1037 variables of tropical-forest-ecosystem degradation and restoration. *Forests* 14, 586.
1038 <https://doi.org/10.3390/fl4030586>
- 1039 Lewis, S.A., Hudak, A.T., Ottmar, R.D., Robichaud, P.R., Lentile, L.B., Hood, S.M., Cronan,
1040 J.B., Morgan, P., 2011. Using hyperspectral imagery to estimate forest floor consumption
1041 from wildfire in boreal forests of Alaska, USA. *Int. J. Wildland Fire* 20, 255.
1042 <https://doi.org/10.1071/WF09081>
- 1043 Lewis, S.A., Hudak, A.T., Robichaud, P.R., Morgan, P., Satterberg, K.L., Strand, E.K., Smith,
1044 A.M.S., Zamudio, J.A., Lentile, L.B., 2017. Indicators of burn severity at extended
1045 temporal scales: A decade of ecosystem response in mixed-conifer forests of western
1046 Montana. *Int. J. Wildland Fire* 26, 755. <https://doi.org/10.1071/WF17019>



- 1047 Lewis, S.A., Robichaud, P.R., Archer, V.A., Hudak, A.T., Eitel, J.U.H., Strand, E.K., 2023.
1048 Informing sustainable forest management: Remote sensing strategies for assessing soil
1049 disturbance after wildfire and salvage logging. *Forests* 14, 2218.
1050 <https://doi.org/10.3390/f14112218>
- 1051 Lewis, S.A., Robichaud, P.R., Hudak, A.T., Austin, B., Liebermann, R.J., 2012. Utility of
1052 remotely sensed imagery for assessing the impact of salvage logging after forest fires.
1053 *Remote Sensing* 4, 2112–2132. <https://doi.org/10.3390/rs4072112>
- 1054 Llorens, R., Sobrino, J.A., Fernández, C., Fernández-Alonso, J.M., Vega, J.A., 2024. Soil burn
1055 severity assessment using Sentinel-2 and radiometric measurements. *Fire* 7, 487.
1056 <https://doi.org/10.3390/fire7120487>
- 1057 Mallinis, G., Maris, F., Kalinderis, I., Koutsias, N., 2009. Assessment of post-fire soil erosion
1058 risk in fire-affected watersheds using remote sensing and GIS. *GIScience & Remote*
1059 *Sensing* 46, 388–410. <https://doi.org/10.2747/1548-1603.46.4.388>
- 1060 Marcos, E., Fernández-García, V., Fernández-Manso, A., Quintano, C., Valbuena, L., Tárrega,
1061 R., Luis-Calabuig, E., Calvo, L., 2018. Evaluation of Composite Burn Index and Land
1062 Surface Temperature for Assessing Soil Burn Severity in Mediterranean Fire-Prone Pine
1063 Ecosystems. *Forests* 9, 494. <https://doi.org/10.3390/f9080494>
- 1064 Marra, E., Cambi, M., Fernandez-Lacruz, R., Giannetti, F., Marchi, E., Nordfjell, T., 2018.
1065 Photogrammetric estimation of wheel rut dimensions and soil compaction after increasing
1066 numbers of forwarder passes. *Scandinavian Journal of Forest Research* 33, 613–620.
1067 <https://doi.org/10.1080/02827581.2018.1427789>



- 1068 Marra, E., Wictorsson, R., Bohlin, J., Marchi, E., Nordfjell, T., 2021. Remote measuring of the
1069 depth of wheel ruts in forest terrain using a drone. *International Journal of Forest*
1070 *Engineering* 32, 224–234. <https://doi.org/10.1080/14942119.2021.1916228>
- 1071 Maurya, S., Abraham, J.S., Somasundaram, S., Toteja, R., Gupta, R., Makhija, S., 2020.
1072 Indicators for assessment of soil quality: a mini-review. *Environ Monit Assess* 192, 604.
1073 <https://doi.org/10.1007/s10661-020-08556-z>
- 1074 Melaas, E.K., Sulla-Menashe, D., Gray, J.M., Black, T.A., Morin, T.H., Richardson, A.D.,
1075 Friedl, M.A., 2016. Multisite analysis of land surface phenology in North American
1076 temperate and boreal deciduous forests from Landsat. *Remote Sensing of Environment*
1077 186, 452–464. <https://doi.org/10.1016/j.rse.2016.09.014>
- 1078 Melendy, L., Hagen, S.C., Sullivan, F.B., Pearson, T.R.H., Walker, S.M., Ellis, P., Kustiyo,
1079 Sambodo, A.K., Roswintiarti, O., Hanson, M.A., Klassen, A.W., Palace, M.W., Braswell,
1080 B.H., Delgado, G.M., 2018. Automated method for measuring the extent of selective
1081 logging damage with airborne LiDAR data. *ISPRS Journal of Photogrammetry and*
1082 *Remote Sensing* 139, 228–240. <https://doi.org/10.1016/j.isprsjprs.2018.02.022>
- 1083 Mesa-Mingorance, J.L., Ariza-López, F.J., 2020. Accuracy Assessment of Digital Elevation
1084 Models (DEMs): A Critical Review of Practices of the Past Three Decades. *Remote*
1085 *Sensing* 12, 2630. <https://doi.org/10.3390/rs12162630>
- 1086 Massicotte P., 2025. *rnatuarearth*: World Map Data from Natural Earth. R package.
1087 DOI:10.32614/CRAN.package.rnatuarearth. URL [https://cran.r-](https://cran.r-project.org/web/packages/rnatuarearth/index.html)
1088 [project.org/web/packages/rnatuarearth/index.html](https://cran.r-project.org/web/packages/rnatuarearth/index.html)



- 1089 Mohieddinne, H., Brasseur, B., Gallet-Moron, E., Lenoir, J., Spicher, F., Kobaissi, A., Horen, H.,
1090 2023. Assessment of soil compaction and rutting in managed forests through an airborne
1091 LiDAR technique. *Land Degrad Dev* 34, 1558–1569. <https://doi.org/10.1002/ldr.4553>
- 1092 Mohieddinne, H., Brasseur, B., Spicher, F., Gallet-Moron, E., Buridant, J., Kobaissi, A., Horen,
1093 H., 2019. Physical recovery of forest soil after compaction by heavy machines, revealed
1094 by penetration resistance over multiple decades. *Forest Ecology and Management* 449,
1095 117472. <https://doi.org/10.1016/j.foreco.2019.117472>
- 1096 Moody, J.A., Shakesby, R.A., Robichaud, P.R., Cannon, S.H., Martin, D.A., 2013. Current
1097 research issues related to post-wildfire runoff and erosion processes. *Earth-Science*
1098 *Reviews* 122, 10–37. <https://doi.org/10.1016/j.earscirev.2013.03.004>
- 1099 Morgan, P., Keane, R.E., Dillon, G.K., Jain, T.B., Hudak, A.T., Karau, E.C., Sikkink, P.G.,
1100 Holden, Z.A., Strand, E.K., 2014. Challenges of assessing fire and burn severity using
1101 field measures, remote sensing and modelling. *Int. J. Wildland Fire* 23, 1045.
1102 <https://doi.org/10.1071/WF13058>
- 1103 NASA Earth Science Technology Office, 2024. ESTO annual report 2024. National Aeronautics
1104 and Space Administration.
- 1105 Nevalainen, P., Salmivaara, A., Ala-Ilomäki, J., Launiainen, S., Hiedanpää, J., Finér, L.,
1106 Pahikkala, T., Heikkonen, J., 2017. Estimating the rut depth by UAV photogrammetry.
1107 *Remote Sensing* 9, 1279. <https://doi.org/10.3390/rs9121279>
- 1108 Paré, D., Bognounou, F., Emilson, E.J.S., Laganière, J., Leach, J., Mansuy, N., Martineau, C.,
1109 Norris, C., Venier, L., Webster, K., 2024. Connecting forest soil properties with
1110 ecosystem services: Toward a better use of digital soil maps—A review. *Soil Science Soc*
1111 *of Amer J* 88, 981–999. <https://doi.org/10.1002/saj2.20705>



- 1112 Pastore, M.A., Lang, A.K., Shaw, J.D., Cahoon, S.M.P., Peter-Contesse, H., Owen, S.M., Morin,
1113 R.S., Knott, J.A., Domke, G.M., Esham, B., Berryman, E.M., 2025. Beneath the surface:
1114 A 25-year review of soil monitoring in the U.S. Forest Inventory and Analysis program.
1115 Forest Ecology and Management 595, 123023.
1116 <https://doi.org/10.1016/j.foreco.2025.123023>
- 1117 Pebesma E., 2018. Simple Features for R: Standardized Support for Spatial Vector Data. The R
1118 Journal 10:1, 439-446.
- 1119 Pellegrini, A.F.A., Harden, J., Georgiou, K., Hemes, K.S., Malhotra, A., Nolan, C.J., Jackson,
1120 R.B., 2021. Fire effects on the persistence of soil organic matter and long-term carbon
1121 storage. Nat. Geosci. 15, 5–13. <https://doi.org/10.1038/s41561-021-00867-1>
- 1122 Perbet, P., Guindon, L., Côté, J.-F., Béland, M., 2025. Evaluating landsat time series of above-
1123 ground biomass to monitor boreal forest recovery following different types of
1124 disturbance. Canadian Journal of Remote Sensing 51, 2587489.
1125 <https://doi.org/10.1080/07038992.2025.2587489>
- 1126 Pierzchała, M., Talbot, B., Astrup, R., 2016. Measuring wheel ruts with close-range
1127 photogrammetry. Forestry 89, 383–391. <https://doi.org/10.1093/forestry/cpw009>
- 1128 Pierzchała, M., Talbot, B., Astrup, R., 2014. Estimating soil displacement from timber extraction
1129 trails in steep terrain: Application of an unmanned aircraft for 3D modelling. Forests 5,
1130 1212–1223. <https://doi.org/10.3390/f5061212>
- 1131 Puliti, S., Saarela, S., Gobakken, T., Ståhl, G., Næsset, E., 2018. Combining UAV and Sentinel-2
1132 auxiliary data for forest growing stock volume estimation through hierarchical model-
1133 based inference. Remote Sensing of Environment 204, 485–497.
1134 <https://doi.org/10.1016/j.rse.2017.10.007>



- 1135 Quintano, C., Fernández-Manso, A., Calvo, L., Roberts, D.A., 2019. Vegetation and Soil Fire
1136 Damage Analysis Based on Species Distribution Modeling Trained with Multispectral
1137 Satellite Data. *Remote Sensing* 11, 1832. <https://doi.org/10.3390/rs11151832>
- 1138 R Core Team, 2024. R: A Language and Environment for Statistical Computing. R Foundation
1139 for Statistical Computing, Vienna, Austria.
- 1140 Rengers, F.K., Tucker, G.E., Moody, J.A., Ebel, B.A., 2016. Illuminating wildfire erosion and
1141 deposition patterns with repeat terrestrial LiDAR. *JGR Earth Surface* 121, 588–608.
1142 <https://doi.org/10.1002/2015JF003600>
- 1143 Robichaud, P.R., Lewis, S.A., Brown, R.E., Bone, E.D., Brooks, E.S., 2020. Evaluating post-
1144 wildfire logging-slash cover treatment to reduce hillslope erosion after salvage logging
1145 using ground measurements and remote sensing. *Hydrological Processes* 34, 4431–4445.
1146 <https://doi.org/10.1002/hyp.13882>
- 1147 Robichaud, P.R., Lewis, S.A., Laes, D.Y.M., Hudak, A.T., Kokaly, R.F., Zamudio, J.A., 2007.
1148 Postfire soil burn severity mapping with hyperspectral image unmixing. *Remote Sensing*
1149 *of Environment* 108, 467–480. <https://doi.org/10.1016/j.rse.2006.11.027>
- 1150 Rose, M.B., Nagle, N.N., 2021. Characterizing Forest Dynamics with Landsat-Derived
1151 Phenology Curves. *Remote Sensing* 13, 267. <https://doi.org/10.3390/rs13020267>
- 1152 Schoenholtz, S.H., Miegroet, H.V., Burger, J.A., 2000. A review of chemical and physical
1153 properties as indicators of forest soil quality: challenges and opportunities. *Forest*
1154 *Ecology and Management* 138, 335–356. [https://doi.org/10.1016/S0378-1127\(00\)004230](https://doi.org/10.1016/S0378-1127(00)004230)
- 1155 Shakesby, R.A., Chafer, C.J., Doerr, S.H., Blake, W.H., Wallbrink, P., Humphreys, G.S.,
1156 Harrington, B.A., 2003. Fire severity, water repellency characteristics and



- 1157 hydrogeomorphological changes following the Christmas 2001 Sydney forest fires.
1158 Australian Geographer 34, 147–175. <https://doi.org/10.1080/00049180301736>
- 1159 Stray, B., Lamb, A., Kaushik, A., Vovrosh, J., Rodgers, A., Winch, J., Hayati, F., Boddice, D.,
1160 Stabrawa, A., Niggebaum, A., Langlois, M., Lien, Y.-H., Lellouch, S., Roshanmanesh,
1161 S., Ridley, K., De Villiers, G., Brown, G., Cross, T., Tuckwell, G., Faramarzi, A., Metje,
1162 N., Bongs, K., Holynski, M., 2022. Quantum sensing for gravity cartography. Nature
1163 602, 590–594. <https://doi.org/10.1038/s41586-021-04315-3>
- 1164 Talbot, B., Astrup, R., 2021. A review of sensors, sensor-platforms and methods used in 3D
1165 modelling of soil displacement after timber harvesting. Croat. j. for. eng. (Online) 42,
1166 149–164. <https://doi.org/10.5552/crojfe.2021.837>
- 1167 Talbot, B., Rahlf, J., Astrup, R., 2018. An operational UAV-based approach for stand-level
1168 assessment of soil disturbance after forest harvesting. Scandinavian Journal of Forest
1169 Research 33, 387–396. <https://doi.org/10.1080/02827581.2017.1418421>
- 1170 Tarun Kshatriya, T., Thamizh Vendan, R., 2025. Emerging Role of Hyperspectral Remote
1171 Sensing in Predictive Soil Health Monitoring Under Climate-Induced Stress Scenarios.
1172 Int. J. Environ. Clim. Change. 15, 170–178. <https://doi.org/10.9734/ijecc/2025/v15i64881>
- 1173 Venanzi, R., Latterini, F., Civitaresse, V., Picchio, R., 2023. Recent applications of smart
1174 technologies for monitoring the sustainability of forest operations. Forests 14, 1503.
1175 <https://doi.org/10.3390/f14071503>
- 1176 Vepakomma, U., Cormier, D., Hansson, L., Talbot, B., 2023. Remote Sensing at Local Scales for
1177 Operational Forestry, in: Girona, M.M., Morin, H., Gauthier, S., Bergeron, Y. (Eds.),
1178 Boreal Forests in the Face of Climate Change, Advances in Global Change Research.



- 1179 Springer International Publishing, Cham, pp. 657–682. <https://doi.org/10.1007/978-3->
1180 031-15988-6_27
- 1181 Veraverbeke, S., Dennison, P., Gitas, I., Hulley, G., Kalashnikova, O., Katagis, T., Kuai, L.,
1182 Meng, R., Roberts, D., Stavros, N., 2018. Hyperspectral remote sensing of fire: State-of-
1183 the-art and future perspectives. *Remote Sensing of Environment* 216, 105–121.
1184 <https://doi.org/10.1016/j.rse.2018.06.020>
- 1185 Weiss, M., Jacob, F., Duveiller, G., 2020. Remote sensing for agricultural applications: A meta-
1186 review. *Remote Sensing of Environment* 236, 111402.
1187 <https://doi.org/10.1016/j.rse.2019.111402>
- 1188 White, J.C., 2024. Characterizing forest recovery following stand-replacing disturbances in
1189 boreal forests: contributions of optical time series and airborne laser scanning data. *Silva*
1190 *Fenn* 58. <https://doi.org/10.14214/sf.23076>
- 1191 White, J.C., Wulder, M.A., Hermosilla, T., Coops, N.C., Hobart, G.W., 2017. A nationwide
1192 annual characterization of 25 years of forest disturbance and recovery for Canada using
1193 Landsat time series. *Remote Sensing of Environment* 194, 303–321.
1194 <https://doi.org/10.1016/j.rse.2017.03.035>
- 1195 Whitman, E., Parisien, M.-A., Holsinger, L.M., Park, J., Parks, S.A., 2020. A method for
1196 creating a burn severity atlas: An example from Alberta, Canada. *Int. J. Wildland Fire* 29,
1197 995. <https://doi.org/10.1071/WF19177>
- 1198 Wickham, H., 2010. stringr: Modern, consistent string processing. *The R Journal*, 2(2), 51-
1199 55. <https://journal.r-project.org/articles/RJ-2010-012/>.
- 1200 Wickham H., 2016. *ggplot2: Elegant Graphics for Data Analysis*. Springer-Verlag New York.
1201 ISBN 978-3-319-24277-4, <https://ggplot2.tidyverse.org>



1202 Wickham, H., Averick, M., Bryan, J., Chang, W., McGowan, L.D., François, R., Golemund, G.,
1203 Hayes, A., Henry, L., Hester, J., Kuhn, M., Pedersen, T.L., Miller, E., Bache, S.M.,
1204 Müller, K., Ooms, J., Robinson, D., Seidel, D.P., Spinu, V., Takahashi, K., Vaughan, D.,
1205 Wilke, C., Woo, K., Yutani, H., 2019. Welcome to the tidyverse. *Journal of Open Source*
1206 *Software* 4, 1686. <https://doi.org/10.21105/joss.01686>

1207 Wickham H., 2025a. forcats: Tools for Working with Categorical Variables (Factors). R package
1208 version 1.0.1, <https://forcats.tidyverse.org/>.

1209 Wickham H., Pedersen T., Seidel D., 2025b. scales: Scale Functions for Visualization. R package
1210 version 1.4.0, <https://scales.r-lib.org>

1211 Yu, H., Kong, B., Wang, Q., Liu, Xian, Liu, Xiangmeng, 2020. Hyperspectral remote sensing
1212 applications in soil: a review, in: *Hyperspectral Remote Sensing*. Elsevier, pp. 269–291.
1213 <https://doi.org/10.1016/B978-0-08-102894-0.00011-5>
1214